

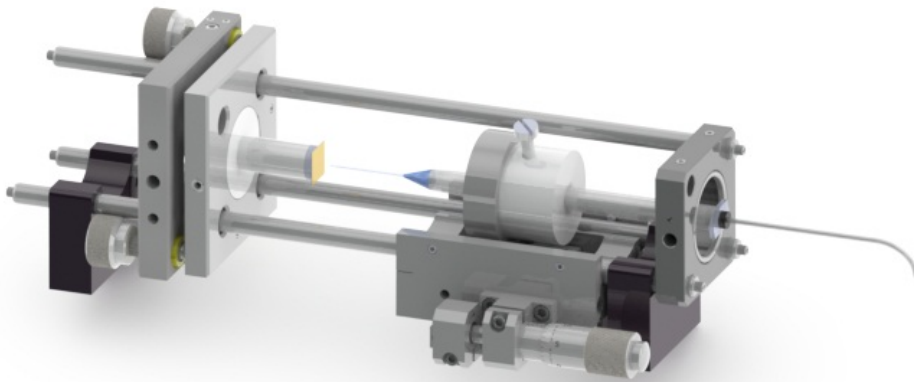
UNIVERSITY OF TWENTE

EEMCS - Electrical Engineering  
Transducers Science and Technology

---

## Electrospray from glass capillaries

---



**Joël van Tiem**

BSc report  
Advanced Technology

**Supervisors**

dr. ir. N.R. TAS  
ir. J. GEERLINGS  
dr. R.M.J. VAN DAMME

July 1, 2012

## Abstract

Electrospray from glass capillaries with 10 and 1  $\mu\text{m}$  diameter apertures at 10 to 30  $\mu\text{m}$  capillary-electrode distances has been performed. Electrospray denotes the process in which subjecting a liquid to high potentials leads to ejecting a small jet and finally dispersal of the liquid. Among the various applications of electrospray are soft ionization techniques and micro- and nano droplet fabrication. Interest lies in the miniaturization of the spraying process without suffering from electrical breakdown by reducing the applied voltages. This can be achieved by reducing the capillary-electrode distance. Another approach would be increasing the pressure applied to the capillary. Both methods have been studied. Focus lies on the design, construction and testing of a setup which is able to perform electrospray from apertures with 100 nm to 10  $\mu\text{m}$  diameter. The setup provides a safe environment in which the electrospray process can be studied precisely. Among the most important characteristics is the ability to tune and measure the capillary-electrode distance very accurately. Results from measurements with 1  $\mu\text{m}$  apertures at a capillary-electrode distance of 10  $\mu\text{m}$  show electrospray is possible using sub kilovolt potentials. Optical analysis verify actual electrospray rather than just electrical breakdown takes place in this configuration. Increasing pressure or decreasing capillary-electrode distances proved to reduce the voltage needed to start the spraying.

# Contents

<b>1</b>	<b>Introduction</b>	<b>3</b>
1.1	Assignment . . . . .	3
1.2	Brief overview of the electrospray process . . . . .	3
<b>2</b>	<b>Theoretical background</b>	<b>7</b>
2.1	Electric field and onset voltage . . . . .	7
2.2	Generation of gas phase ions . . . . .	10
2.2.1	Ion Evaporation Model (IEM) . . . . .	11
2.3	Current . . . . .	12
2.4	Electrical Breakdown . . . . .	13
2.5	Parameter effects . . . . .	17
2.5.1	Conductivity . . . . .	17
2.5.2	Viscosity . . . . .	18
2.5.3	Flow rate . . . . .	18
2.6	Laplace pressure . . . . .	19
2.7	Capillary flow resistance . . . . .	21
2.7.1	Capacitance . . . . .	22
2.8	Modes . . . . .	24
<b>3</b>	<b>Method</b>	<b>26</b>
3.1	Electrospray setup . . . . .	26
3.1.1	Tip-electrode distance . . . . .	29
3.1.2	Angular rotations . . . . .	31
3.1.3	Filling and filtering . . . . .	36
3.1.4	Schematic representation . . . . .	40
3.2	Suitable liquids . . . . .	41
3.3	Flow resistance measurement . . . . .	43
<b>4</b>	<b>Results</b>	<b>45</b>
4.1	Flow resistance . . . . .	45
4.2	Counter electrode . . . . .	48
4.3	Conductivity measurement . . . . .	49
4.4	Electrospray . . . . .	51

4.4.1	Reference measurements . . . . .	51
4.4.2	Fluid measurements . . . . .	55
4.4.3	Fluid pressure measurements . . . . .	59
<b>5</b>	<b>Data analysis</b>	<b>79</b>
<b>6</b>	<b>Conclusions</b>	<b>83</b>
<b>7</b>	<b>Discussion and recommendations</b>	<b>84</b>
<b>8</b>	<b>Appendices</b>	<b>91</b>

# Chapter 1

## Introduction

### 1.1 Assignment

The main goal of this study is to build a setup for electrospray from glass capillaries. Capillaries with apertures from 100 nm to 10  $\mu\text{m}$  are commercially available. Interest lies in the question whether it is possible to perform electrospray from these apertures at low voltages (i.e. smaller than 100 V) by bringing the capillary close to the counter electrode (10 - 50  $\mu\text{m}$ ). Among the experimental challenges are the accurate positioning of the capillary, measurement of the gap spacing and the possible electric breakdown in the air gap.

### 1.2 Brief overview of the electrospray process

Electrospray denotes the process in which a high voltage (typically in the range of 1 - 5 kV<sup>1</sup>) is applied to a liquid and a grounded electrode in order to disperse the liquid. Very low flow rates of 1 to 10  $\mu\text{l min}^{-1}$  are common.<sup>2</sup> In this study the liquid is supplied in a glass capillary with apertures of 100 nm to 10  $\mu\text{m}$ . The electric field induced by the applied voltage causes charges to migrate towards the tip of the meniscus (positive charges if the applied voltage is positive).<sup>3</sup> If the effects of gravity are neglected, an equilibrium state will be set when the surface tension equals the tension induced by the applied voltage, the so called Maxwell stress.<sup>24</sup> A simplified setup is shown in Figure 1.1.

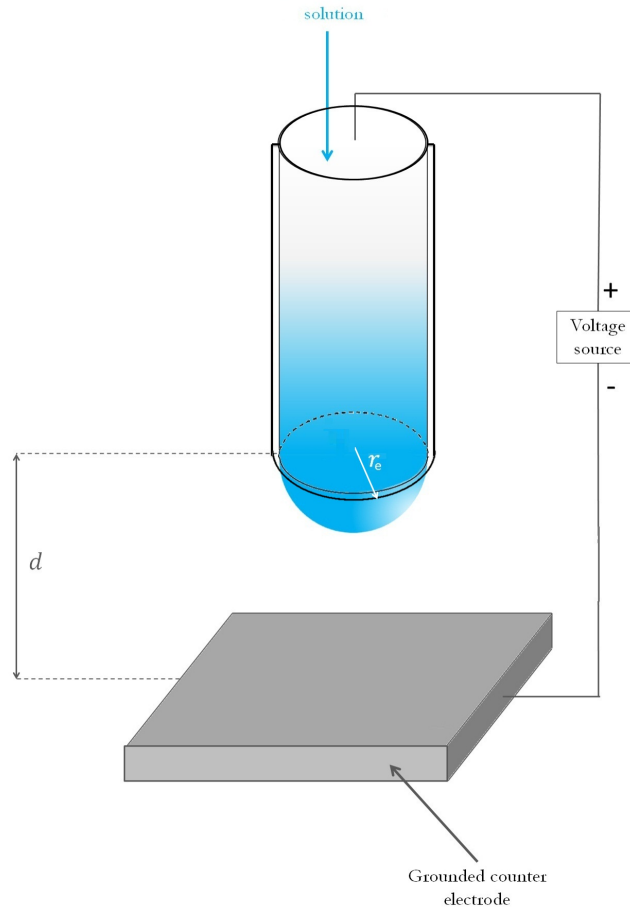


**Figure 1.1** – Simplified electro spray setup. Note the distance ratios are not scaled. Typical tip-electrode distances  $d$  are 10 - 100  $\mu\text{m}$ , aperture diameters range from 100 nm - 10  $\mu\text{m}$ .

As described by Taylor, in this equilibrium state ideally a *Taylor cone* with a middle half angle of  $\theta_T = 49.3^\circ$  arises.<sup>5</sup> Now equilibrium is no longer preserved which causes the angle to decrease slightly and the flow rate to increase.<sup>2</sup> A jet through the apex of the cone is produced. This is illustrated by Figure 1.2.

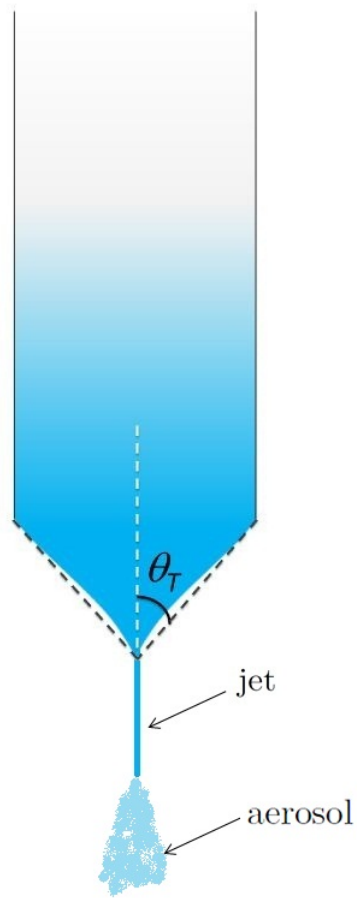


**Figure 1.2** – A capillary in spraying mode. A jet leaves the tip of the cone which eventually breaks up into an aerosol.

A certain voltage has to be applied before the Taylor cone arises (see Figure 1.3).

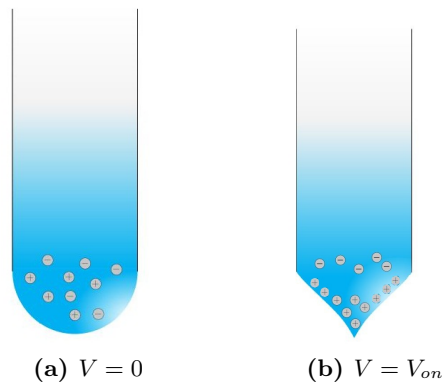


**Figure 1.3** – The meniscus is changing when a voltage  $V$  is applied. At (a) no voltage is applied and an ordinary meniscus without charge migration occurs. If  $V$  increases up to the onset voltage  $V_{on}$  a Taylor cone arises and positive charges are pushed towards the apex of the cone.

If the applied voltage exceeds the onset voltage a jet will be created which breaks up into an aerosol. Main applications are found in the field of mass spectrometry<sup>1</sup> and micro- and nano-thin-film deposition.<sup>6</sup> Electrospray for ionization (ESI) is, among other applications, ideal for biochemical analyses since relatively large biomolecules can be studied using mass spectrometry.<sup>7</sup> Applications are also found in the production of micro- and nanometer droplets.<sup>8</sup>

## Chapter 2

# Theoretical background

Previous work (refer to e.g. Wilm,<sup>2</sup> Taylor,<sup>5</sup> Kebarle<sup>9</sup>) has shown theoretical models are able to predict experimental results quite accurately. Therefore it is useful to consider these models. Especially expressions for the onset voltage, current and breakdown voltage as a function of given parameters are extremely useful.

### 2.1 Electric field and onset voltage

If a static situation (i.e. the situation *before* the actual spraying begins) is considered the force induced by the electric field will pull the liquid outwards whilst the surface tension is pushing the liquid back in since it tries to minimize the surface. Making two assumptions makes it possible to derive an expression for the Taylor angle  $\theta_T$ :<sup>3</sup>

$$P_{1/2}(\cos(\theta)) = 0 \tag{2.1}$$

In which  $P_{1/2}(\cos(\theta))$  denotes the *Legendre polynomial* of order 1/2 as a function of  $\cos(\theta)$ , i.e. the solution to Equation 2.2

$$\frac{d}{d(\cos(\theta))} \left[ (1 - (\cos(\theta))^2) \frac{d}{d(\cos(\theta))} P_{1/2}(\cos(\theta)) \right] \frac{1}{2} \left( \frac{1}{2} + 1 \right) P_{1/2}(\cos(\theta)) = 0 \tag{2.2}$$

This expression only holds if (1) a static situation for all points is assumed. This results in the Legendre polynomial having order 1/2. Next, an equipotential liquid surface with the electric field perpendicular to it has to be assumed (2). This causes the  $P_{1/2}(\cos(\theta))$  term to equal zero.<sup>2</sup>

Solving Equation 2.1 yields the Taylor cone angle of  $\theta_T = 49,3^\circ$ . The total derivation is performed by Wilm.<sup>2</sup> As demonstrated by Smith<sup>10</sup> the surface of the cone is not really equipotential. However, this model provides rather accurate predictions. Under this assumption an expression for the electric field  $\vec{E}$  at the tip induced by the voltage  $V$  can be derived:

$$|\vec{E}| = A \left( \frac{V}{r_e \ln \frac{4d}{r_e}} \right) \quad (2.3)$$

In which  $r_e$  denotes the capillary radius and  $d$  the capillary - counter electrode distance. Note in this equation the capillary radius has been equated to the aperture radius and it only holds under the assumption that  $d \gg r_e$ . Jones,<sup>11</sup> Loeb<sup>12</sup> and Taylor<sup>5</sup> derived all three the same expression, except the variable  $A$ . Loeb and Rohner give  $A = 2$  whilst Jones gives  $A = \sqrt{2}$ . However, as this is only a scaling factor, the behavior of the electric field as a function of the capillary radius and voltage can be studied. Reasonable values in this study have been plotted in Figure 2.1 ( $r_e \in [0.1, 10] \mu m, V \in [0, 5] kV$ ).

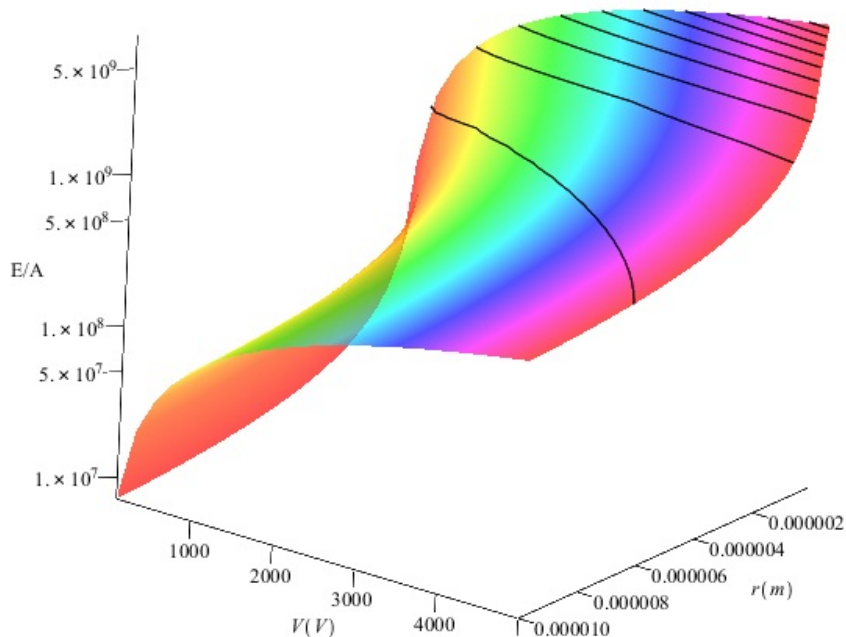


**Figure 2.1** – Plot of the normalized electric field as a function of voltage  $V$  and capillary radius. A tip-electrode distance  $d$  of  $10\mu m$  has been used. The color refers to the value of  $V$  and the black lines are electric field iso lines.

In order to create an equilibrium state between the Maxwell stress (which

reads  $\frac{1}{2}\epsilon_0 E^2$ )<sup>13</sup> and surface tension an onset voltage  $V_{on}$  has to be applied. This voltage can be seen as a boundary between equilibrium and instability. Equating both terms yields a very useful expression for the required onset voltage as a function of surface tension  $\gamma$ , capillary radius  $r_e$  and tip-electrode distance  $d$ :<sup>10</sup>

$$V_{on} = A \sqrt{\frac{2\gamma r_e \cos(\theta_T)}{\epsilon_0}} \ln\left(\frac{4d}{r_e}\right) \quad (2.4)$$

Reasonable values like in Figure 2.1 have been plotted in Figure 2.2. A surface tension of  $\gamma = 22.6 \cdot 10^3 \text{ N}\mu\text{m}^{-1}$  has been used in this example. This is a reasonable value as this equals the surface tension of methanol which is commonly used in electrospray.<sup>9</sup>

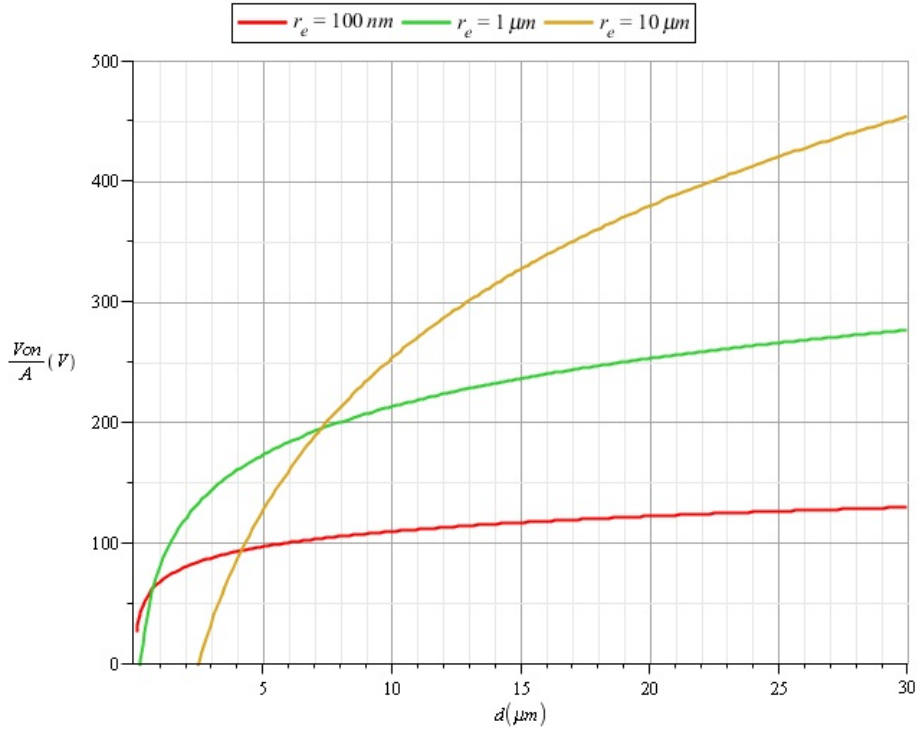


**Figure 2.2** – In order to study the effects of  $d$  and  $r_e$  on the onset voltage qualitatively without concerning  $A$ ,  $\frac{V_{on}}{A}$  has been plotted. Note that  $r_e$  refers to the radius of the capillary. In this study capillaries with a *diameter* of 0.1, 1 and 10  $\mu\text{m}$  are used.

## 2.2 Generation of gas phase ions

When the jet has created an aerosol the solvent will start to evaporate. This evaporation will cause the created droplets to shrink. As the total charge inside the droplets is preserved, the charge density increases. Due to the Coulomb force  $\vec{F}_c$ , which reads

$$\vec{F}_c = \frac{q_1 q_2}{4\pi\epsilon_0 |\vec{r}_1 - \vec{r}_2|^3} (\vec{r}_1 - \vec{r}_2) \quad (2.5)$$

repulsion of charges will increase. The maximum charge  $q$  at which a droplet with radius  $r$  is stable is described by the Rayleigh limit:<sup>14</sup>

$$q^2 = 64\pi^2\epsilon_0\gamma r^3 \quad (2.6)$$

If this limit is exceeded droplets will explode causing a *jet-fission*. Next, ions will be guided to the counter electrode by the electric field. The generation process of these ions is still not well understood. Two theories have been proposed.<sup>3</sup>

First, the ion evaporation model (IEM) states the forces inside the droplet are strong enough to lift an ion 'directly' from the droplet. It is assumed that in order to do this, the droplet first has to shrink (by solvent evaporation) to a radius smaller than 10 nm.<sup>15</sup> Second, the charge residue model (CRM)<sup>16</sup> states that a series of fission of droplets takes place. This continues until only droplets with only one charge remain. The solvent is indeed evaporating which increases the Coulombic repulsion. However, the charge per droplet is also decreasing which prevents exceeding the Rayleigh limit. The distinction between the two theories is hard to draw. It is speculated that the IEM particularly applies to small ions whereas the CRM holds for large ions. A schematic overview of the two models is displayed in Figure 2.3.

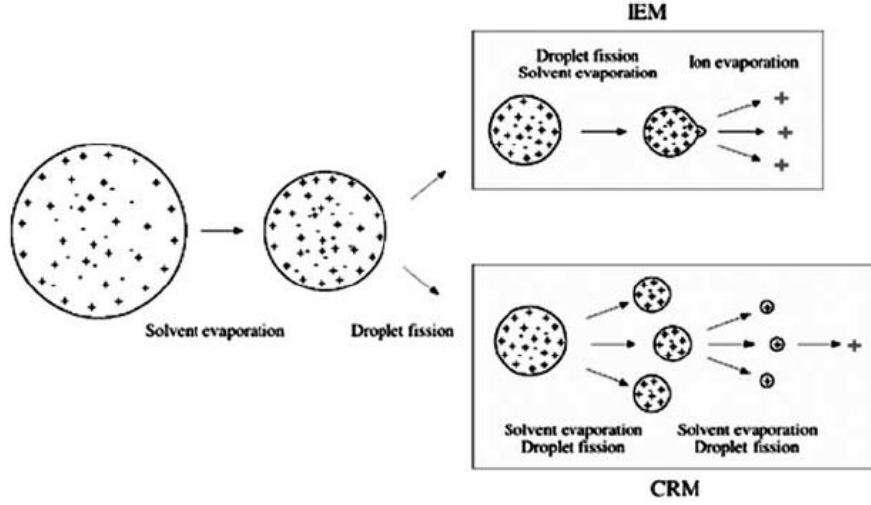


**Figure 2.3** – An overview of the two gas-phase ionization models. Adopted from Rohner<sup>3</sup>

### 2.2.1 Ion Evaporation Model (IEM)

Taking a better look at the IEM the electric field in a droplets induced by the charge inside has to be considered. Gauss' Law reads:

$$\oiint_{\partial A} \vec{E} \cdot \hat{n} \, dS = \frac{\sum q}{\epsilon_0} \quad (2.7)$$

For a point charge, the Gaussian surface equals the surface of a sphere with radius  $r$  and the total charge  $Ze$  in which  $Z$  denotes the number of charges and  $e$  the elementary charge. Therefore, the electric field can be described by

$$|\vec{E}| = \frac{Ze}{4\pi\epsilon_0 r^2} \quad (2.8)$$

If the maximum charge due to the Rayleigh limit is included for  $Ze$  (refer to Equation 2.6) an expression for the maximum electric field in the droplet  $E_m$  is obtained.

$$E_m = 2\sqrt{\frac{\gamma}{\epsilon_0 r}} \quad (2.9)$$

Still, it is very hard to make a clear distinction between the two models as the radii of the droplets are very tiny. However, studies have indicated that the ion evaporation model is the most likely theory (for small ions).<sup>3,15</sup>

## 2.3 Current

As already explained, the applied voltage causes charges to migrate towards the apex of the cone. As long as the voltage does not exceed the onset voltage, a static situation can be treated so there's no 'closed circuit' (This only holds in theory. In section 2.4 the phenomenon of electrical breakdown, which causes a current without exceeding the onset voltage, will be explained in detail). However, if the voltage *does* exceed the onset voltage charges will leave the capillary and go the counter electrode: a current  $i_s$  is created.

Various theories to describe this phenomenon have been proposed. Three important and quite distinct models are discussed. Equation 2.10 has been proposed by Pfeiffer and Hendricks<sup>17</sup>

$$i_s(\epsilon_r, \sigma, \gamma, v_f, E) = \left\{ \left( \frac{4\pi}{\epsilon_r} \right)^3 (9\gamma)^2 \epsilon_0^5 \right\} \sqrt[7]{(\sigma E)^3} \sqrt[7]{v_f^4} \quad (2.10)$$

In which  $\sigma$  denotes the conductivity of the liquid,  $\epsilon_r$  the liquid's relative permittivity and  $v_f$  the flow rate. Note in this model the current depends on five major parameters. Another, more simple relation has been derived by J.F. de la Mora<sup>18</sup> in Equation 2.11

$$i_s(\epsilon_r, \sigma, \gamma, v_f) = f(\epsilon_r) \sqrt{\gamma \sigma v_f \epsilon_r} \quad (2.11)$$

$f(\epsilon_r) \approx 18 \forall \epsilon_r \geq 40$  which is the case for the previously used example methanol. Note there is no electric field dependency in this relationship. For sufficiently high conductivities the electric field can be neglected. Yet another relationship has been proposed by Smith<sup>10</sup>

$$i_s \propto \frac{1}{\rho \sigma} \sqrt{\frac{\gamma^3}{R_j}} \quad (2.12)$$

in which  $\rho$  denotes the density of the liquid and  $R_j$  the radius of the jet. It can be concluded that all three relationships show that the current  $i_s$  depends on both the conductivity  $\sigma$  and surface tension  $\gamma$  of the liquid, which was to be expected. However, the dependences differ quite a lot (refer to Figure 2.5). The dependence of  $R_j$  on  $\sigma$  and  $V$  is not studied. Therefore it is not easy to speculate about the current's dependence on conductivity in the model. Also, Smith is the only one taking the liquid's density into account.

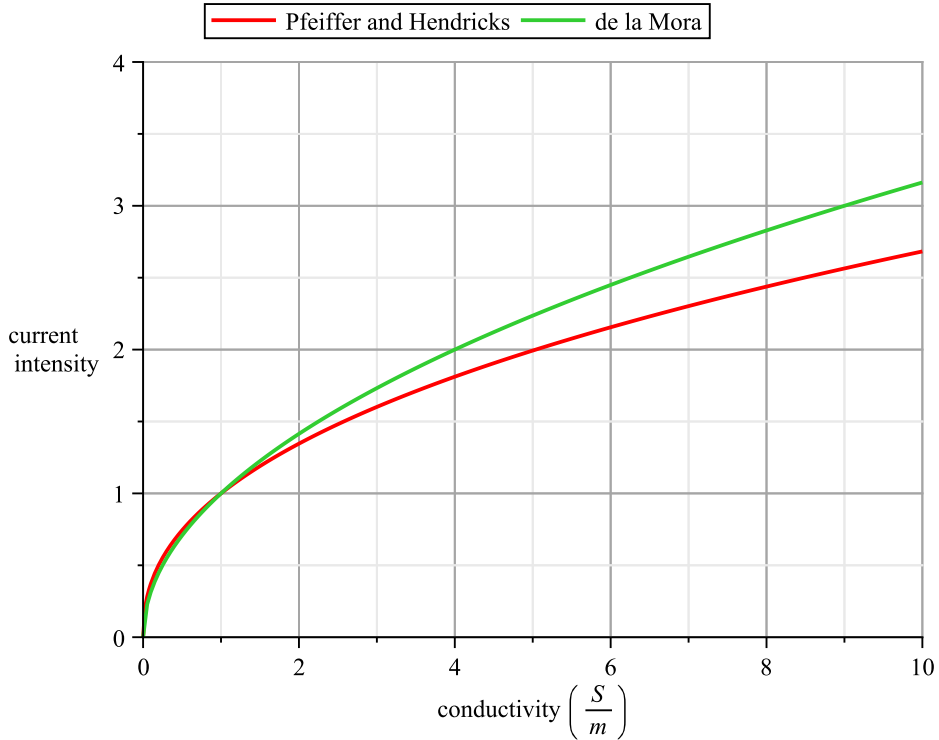


**Figure 2.4** – Plots of the proposed currents depending on conductivity  $\sigma$ . The current proposed by Smith has not been plotted as the dependence of  $R_j$  on  $\sigma$  is not studied.

## 2.4 Electrical Breakdown

Since high voltages and relatively small gap distances are involved in the electro spray process *electrical breakdown* has to be taken into account. Electrical breakdown is the process in which a 'current runs' through a gas when a certain (high) voltage is applied. This phenomenon is usually (especially in small devices) explained by the so called Townsend avalanche gas breakdown.<sup>19</sup> This theory states that breakdown can only occur if free electrons (accelerated by the electric field due to the high applied voltage) have enough energy to ionize atoms after collisions. Due to this ionization another free electron is created and also collides, which causes yet *another* free electron. This process makes the avalanche and will eventually create a spark (i.e. breakdown).

Paschen<sup>20</sup> studied the electrical breakdown between two electrodes. He proposed the famous *Paschen curves* which describe the breakdown voltage as a function of the ambient pressure and gap distance. Using these curves, the minimum voltage at which electrical breakdown occurs can be calculated

and a 'safe zone' can be determined. These predictions also make it possible to tune the pressure (and gap distance, but this is usually constrained) in order to increase the breakdown voltage. Paschen described that at pressure  $p$  and gap distance  $d$  the voltage  $V_b$  at which electrical breakdown occurs reads<sup>21</sup>

$$V_b(p, d) = \frac{Bpd}{\ln(Apd) - \ln(\ln(1 + \frac{1}{\alpha}))} \quad (2.13)$$

in which  $A$  and  $B$  are (more or less) constants which depends on the gas in which the electrodes are placed.<sup>22</sup>  $\alpha$  denotes the so called *second Townsend coefficient*. It can be seen as a gas property. However, in theory it is a little bit more tedious. As described by Burm<sup>22</sup>  $\alpha$  can be described using the Fermi-Dirac distribution. This distribution describes the average occupation number of electrons (or more general *fermions*) in a state  $n$  with energy  $\mathcal{E}_n$   $\langle m_n \rangle$

$$\langle m_n \rangle = f(\mathcal{E}_n) = \frac{1}{\exp\left(\frac{\mathcal{E}_n - E_f}{kT}\right) + 1} \quad (2.14)$$

In which  $T$  denotes the temperature and  $k$  Boltzmann's constant.  $E_f$  denotes the *Fermi level*. This is defined as the energy at which the average occupation number is exactly 0.5, i.e. the chance of an electron with energy  $\mathcal{E}_n$  is found in state  $n$  is exactly 50%. It turns out that  $\alpha$  can be described as

$$\alpha = \frac{1}{E_f} \int_{E_{free}}^{\infty} \frac{1}{\exp\left(\frac{\mathcal{E}_n - E_f}{kT}\right) + 1} d\mathcal{E}_n \quad (2.15)$$

In which  $E_{free}$  denotes the energy at which an electron becomes free. A simplified expression reads

$$\alpha = \frac{kT}{E_f} \exp\left(\frac{-(E_{free} - E_f)}{kT}\right) \quad (2.16)$$

The total derivation if performed by Burm.<sup>22</sup> The gas properties  $A$  and  $B$  are tabulated. An example (air) of the curvature of the Paschen curve is drawn in Equation 2.13.

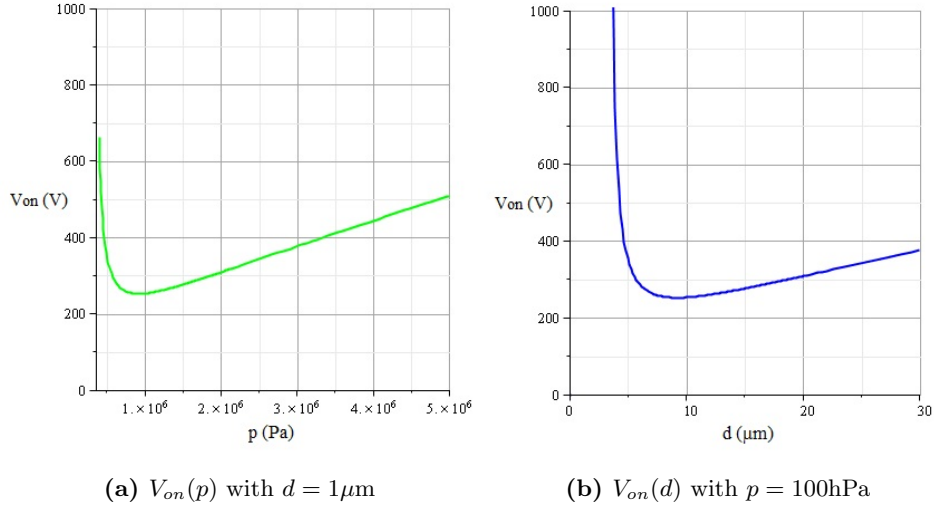


**Figure 2.5** – Example of the Paschen curve. This curve holds for air ( $A = 10.95 \text{ Pa}^{-1} \text{ m}^{-1}$ ,  $B = 273.78 \text{ V Pa}^{-1} \text{ m}^{-1}$  and  $\kappa = 0.025$ ).<sup>22</sup> It can be observed that the minimum breakdown voltage is about 250 V at approximately 10 times atmospheric pressure. On the other hand, at atmospheric pressure breakdown will occur around 250 V with a gap distance of approximately 10  $\mu\text{m}$ .

In order to calculate at what pressure the minimum breakdown voltage occurs the expression can be differentiated and equated to zero, i.e. solving

$$\frac{\partial V_b}{\partial(pd)} = 0 \quad (2.17)$$

This minimum in the Paschen curve corresponds to the state at which electrons just have sufficient energy to ionize an atom (or molecule).

Until now breakdown doesn't look too bad. As indicated by Equation 2.13 the breakdown voltage only increases when going to very small gap distances. And this is more or less true for every day macroscopic applications. Previous work reported strong deviations from the Paschen curves when operating with gaps smaller than 10  $\mu\text{m}$  at approximately atmospheric pressure.<sup>23,24</sup> Figure 2.5 also predicts the validity of the Paschen curves ends somewhere around  $d \approx 500\text{nm}$ . An asymptote can be seen in the Paschen curve there. This singularity rises when the denominator equals zero:

$$\ln(Apd) = \ln \left( \ln \left( 1 + \frac{1}{\alpha} \right) \right) \quad (2.18)$$

$$Apd = \ln \left( 1 + \frac{1}{\alpha} \right) \quad (2.19)$$

$$d = \frac{\ln \left( 1 + \frac{1}{\alpha} \right)}{Ap} \quad (2.20)$$

If small dimensions are reached in e.g. microfluidic devices (like electrospray) another effect has to be taken into account. Some conducting electrons in a metal are close to the surface. If a high voltage is applied to the metal they will be pulled out of the metal (*field emissions*). Field emission has been studied thoroughly, but it will only be explained briefly here. As the electrons are free now, they will accelerate to the counter electrode. Studies have shown that at small distances the field emission process is taking a more important part than the Townsend avalanche effect.<sup>25</sup> In addition to field emission, there is also a region where ion enhanced field emission takes the most important part.<sup>4</sup> The Paschen curve has to be modified to include these phenomena (refer to Figure 2.6 and Figure 2.7).

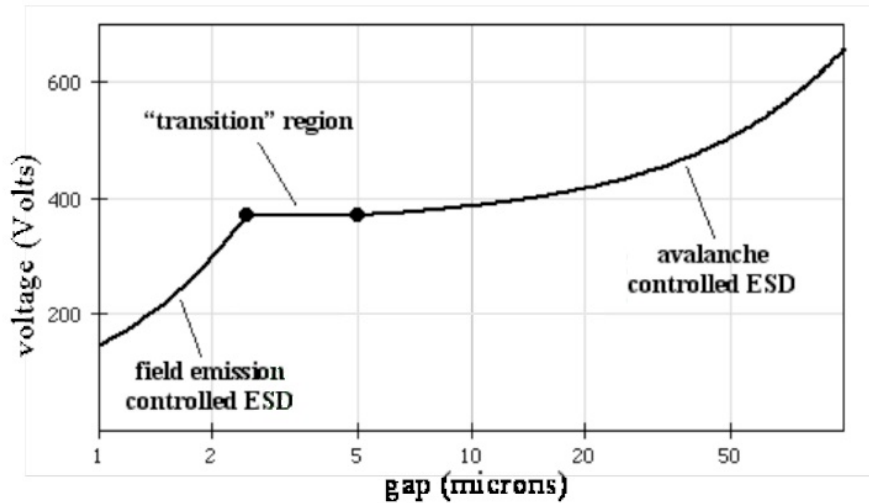


**Figure 2.6** – The modified Paschen curve. The right hand side of the curve ( $d > 5\mu m$ ) shows the traditional Paschen curve. This part of the curve is controlled by Townsend avalanche electrostatic discharge (ESD). Going to smaller gap distances first gives a transition region, but whilst it can be expected the breakdown voltage will increase by the traditional Paschen curve, it's *decreasing* rapidly. This is caused by the field emissions. Adopted from Longwitz.<sup>26</sup>

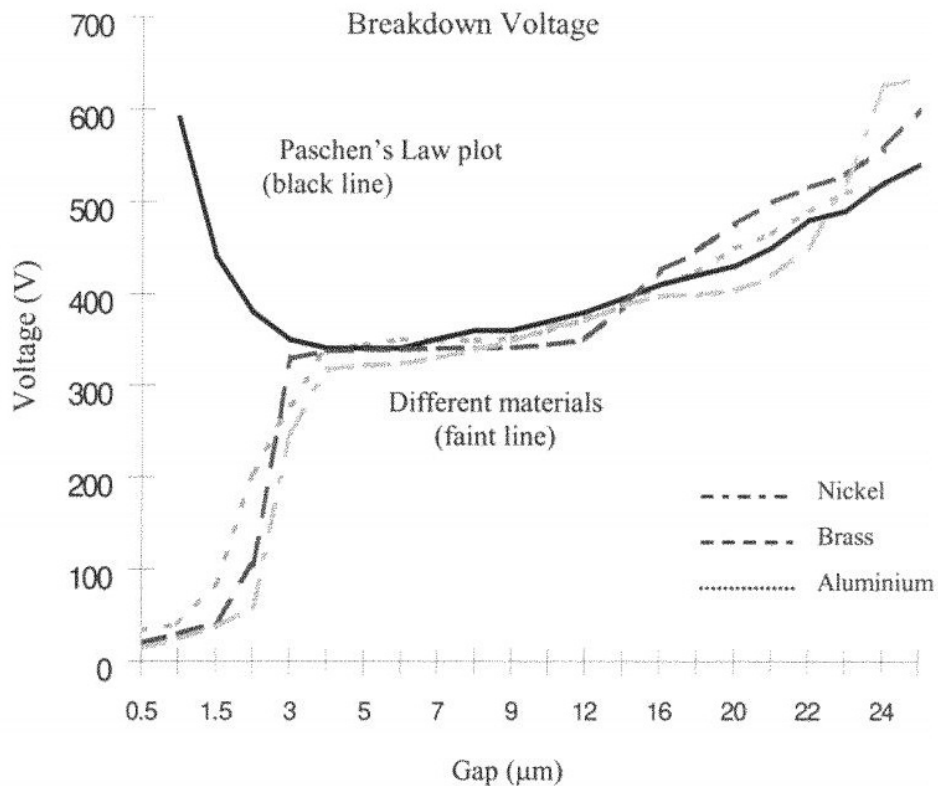


**Figure 2.7** – Breakdown voltage as a function of the gap. Several materials have been used. Unfortunately the breakdown voltage does not increase with decreasing gap, but drops to very low values in the sub  $5 \mu\text{m}$  regime. This can give significant difficulties as this regime will be used in this study. Whereas this plot predicts a breakdown voltage of less than 50 V with a gap distance of about  $1 \mu\text{m}$  it is to be expected that the onset voltage will be somewhat in the range of a couple of hundred Volts (refer to Equation 2.4 and Figure 2.2). Adopted from Torres.<sup>24</sup>

## 2.5 Parameter effects

As discussed in the previous section, several parameters are determining in the electrospray process. For example, the onset voltage and the capillary radius take an important part. But the liquid properties influence the process as well. The surface tension takes a significant part, but also conductivity and viscosity need to be regarded.

### 2.5.1 Conductivity

As predicted in section 2.3 the current strongly depends on the conductivity of the liquid, which is to be expected. Previous work has shown that

at very low conductivities no spraying occurs at all. Various empirical results show almost no conductivity dependence in the onset voltage, just like Equation 2.4.<sup>10</sup> Studies prove that the current increases with increasing conductivity.<sup>10,27</sup>

### 2.5.2 Viscosity

The viscosity of a fluid is a measure for how easy it is to deform the liquid by shear of tensile stress. For instance, it is easier to press water through a small tube than syrup. It can be expected that viscosity does influence the electrospray process. Studies have shown this influence, but mostly in the dynamic behavior of the process.<sup>28</sup> The onset voltage does not change drastically with changing viscosity. In addition, modifying the viscosity while keeping other parameters (conductivity, surface tension etc.) constant proved to be rather hard.<sup>10</sup>

### 2.5.3 Flow rate

As already suggested by Equation 2.10 the flow rate  $v_f$  is also determining for the electrospray process. Barrero and Loscertales derived an expression for the minimum required flowrate  $v_{f,\min}$  at which a cone-jet can occur (refer to section 2.8).<sup>8</sup>

$$v_{f,\min} \approx \frac{\gamma \epsilon_0 \epsilon_r}{\rho \sigma} \quad (2.21)$$

Previous work has proposed a strong relation of the flow rate (among other parameters) with the diameter of an ejected droplet  $\delta$ .<sup>29,18,30</sup>

$$\delta = f \cdot v_f^{\alpha_v} \quad (2.22)$$

$$f(\sigma, \gamma, \rho, \epsilon_0, \epsilon_r) = \alpha_1 \frac{\epsilon_0^{\alpha_\epsilon} \rho^{\alpha_\rho}}{\sigma^{\alpha_\sigma} \gamma^{\alpha_\gamma}} \quad (2.23)$$

The  $\alpha_1$  constant depends on the liquid's permittivity and the other constants  $\alpha$  vary with the author. An overview can be found in Table 2.1. It is interesting to note that de la Mora states  $\alpha_\gamma = \alpha_\rho = 0$  which implies the droplet size is not a function of the liquid's surface tension or density.

	$\alpha_{v_f}$	$\alpha_\epsilon$	$\alpha_\rho$	$\alpha_\gamma$	$\alpha_\sigma$
de la Mora <sup>18</sup>	1/3	1/3	0	0	1/3
Ganan-Calvo <sup>30</sup>	1/2	1/6	1/6	1/6	1/6
Hertman et al. <sup>29</sup>	1/2	1/6	1/6	1/6	1/6

**Table 2.1** – Values of constants according to various authors

This relation has been confirmed by Rohner<sup>3</sup> who states the droplet's diameter reads approximately:

$$\delta \approx 2 \frac{v_f^{1/3} \cdot \epsilon^{1/3}}{\sigma^{1/3}} \quad (2.24)$$

This relation is (qualitatively) very similar to the model proposed by de la Mora.

## 2.6 Laplace pressure

A certain pressure difference with respect to the ambient pressure is needed when a liquid is pushed through a finite diameter tube. This is caused by the non zero surface tension of the liquid. If a pressure is applied a meniscus which is ideally a circle segment (in 3D a sphere segment) will arise at the fluid - air interface. This circle segment has a certain curvature (see Figure 2.8).

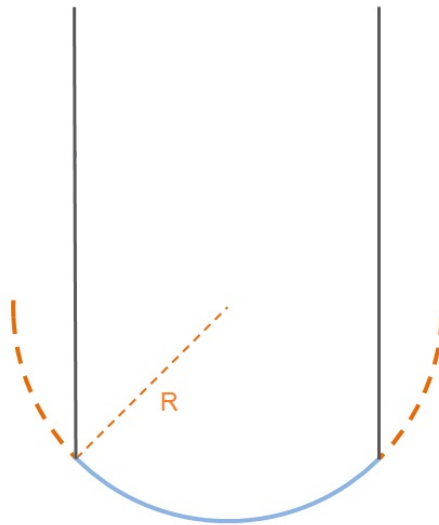


**Figure 2.8** – The meniscus has a spherical interface. If the pressure is increased the curvature  $R$  will decrease.

If the meniscus is assumed to be a perfect sphere segment with a zero thickness interface the pressure difference  $\Delta p$  needed to create a meniscus with curvature  $R$  and surface tension  $\gamma$  reads:<sup>31</sup>

$$\Delta p = \frac{2\gamma}{R} \quad (2.25)$$

This pressure is called the *Laplace pressure*. The maximum Laplace pressure is reached when the meniscus has the form of a sphere segment with a radius equaling the radius of the capillary (refer to 2.9a). The meniscus can increase, but the curvature will increase again. This is demonstrated in Figure 2.9.

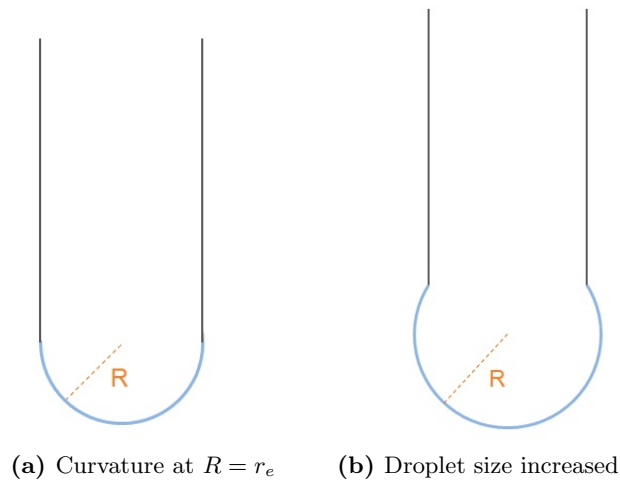
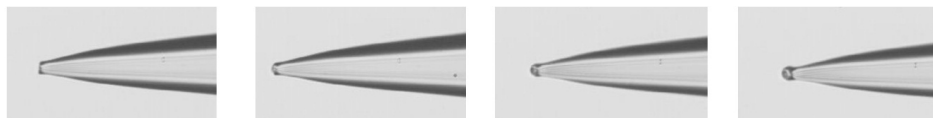


**Figure 2.9** – When the curvature of the meniscus equals the radius of the capillary the Laplace pressure has reached its maximum. So using the capillary radius, which is in most cases a given parameter, the Laplace pressure can be estimated. However, the pressure that has to be applied also depends on the flow resistance of the capillary.



(a) Droplet size with increasing applied pressure from left to right.



(b) Laplace pressure exceeded.

**Figure 2.10** – A (a) the droplet from a 10  $\mu\text{m}$  capillary can be seen. The droplet looks a lot like a sphere, so the spherical shaped meniscus proves to be a good assumption. If the pressure keeps increasing at some point the Laplace pressure will be exceeded by the applied pressure. At this point equilibrium is no longer preserved. The droplet will then come off the capillary, which is shown at (b).

## 2.7 Capillary flow resistance

In addition to the Laplace pressure felt when trying to push a liquid through a tube, also the flow resistance of the tube itself will be felt. It is to be expected that this resistance depends on (among others) the cross sectional area of the tube. If a long (much greater than the capillary radius) capillary with a laminar flow, which is almost always the case in microfluidics, a viscous and incompressible flow and a constant circular cross section is assumed the Hagen-Poiseuille equation describes the flow resistance  $R_V$  as:<sup>32</sup>

$$R_V = \frac{8\mu L}{\pi r^4} \quad (2.26)$$

In which  $\mu$  denotes the (dynamic) viscosity,  $L$  the length of the capillary and  $r$  the capillary radius. The resistance is proportional to  $1/r^4$  which means the resistance is increasing very fast with decreasing radius.

This flow resistance is completely analogous to an electrical resistance. Ohm's Law can therefore also be stated in fluidic terms:

$$\Delta P = Q \cdot R_V \quad (2.27)$$

In which  $Q$  denotes the flow (*current*) and  $\Delta p$  the pressure difference (potential difference, i.e. *voltage*). So the total pressure which has to be applied when pressing a liquid through a capillary is the sum of the Laplace pressure and pressure due to the capillary flow resistance. Note that the Laplace pressure is negative if the capillary has not yet been filled totally (refer to Figure 2.11).

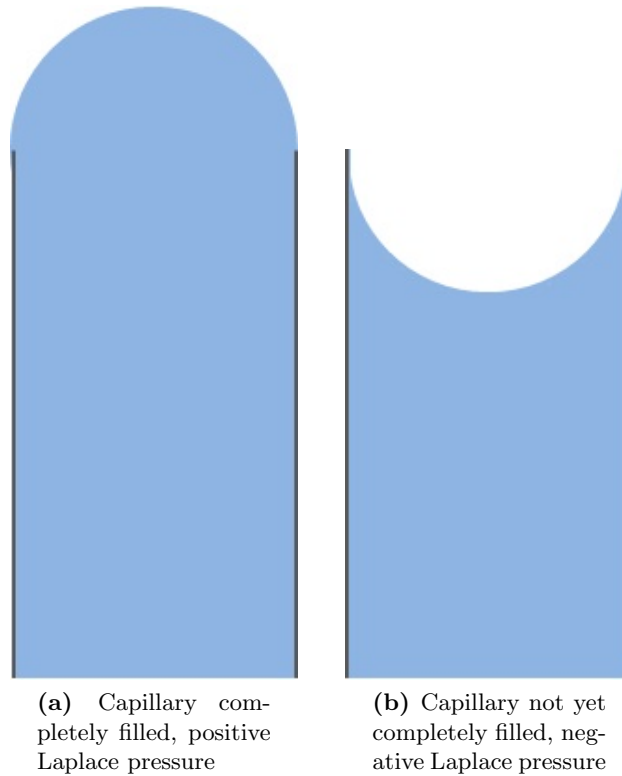


**Figure 2.11** – As shown by the two situations the Laplace pressure is negative if the meniscus is convex instead of concave. The convex shape of the meniscus pulls the liquids 'upwards'.

### 2.7.1 Capacitance

The analogy between an electrical and fluidic network also holds for a capacitor. The fluidic (or hydraulic) capacitance can be described by a tube with a rubber sheet inside (see Figure 2.12): if a certain pressure is applied (*voltage*) a certain volume will flow (*current*) until the rubber sheet is stretched maximally (*capacitor charged*). Energy is stored inside the rubber sheet: it can 'discharge' again if the applied pressure is removed. This is analogous to discharging a capacitor.

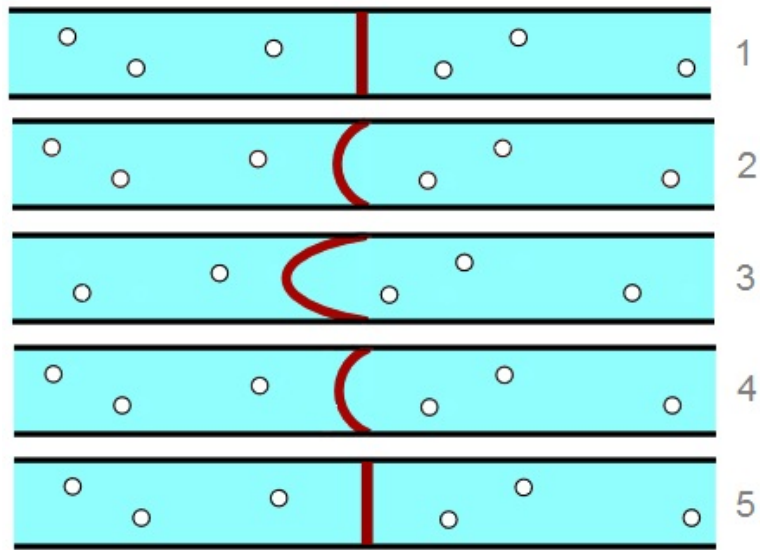


**Figure 2.12** – The rubber is stretched and un-stretched again. This can be seen as analogous to charging and discharging a capacitor.<sup>33</sup>

However, the liquids used in this study are virtually incompressible. Therefore, the actual fluidic capacitance is not so much created by the liquid’s finite compressibility. The fact that especially the tubing can *expand* with changing pressures causes capacitive behavior.

So a capillary has a certain resistance and capacitance. Measuring the pressure as a function of time with a constant flow rate is analogous to the electrical circuit in Figure 2.13.

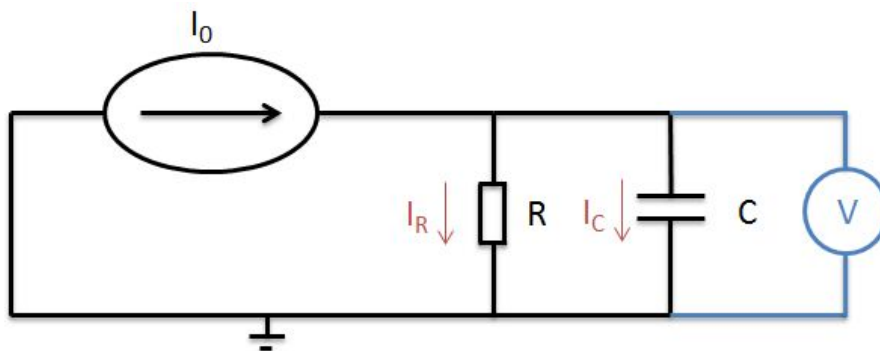


**Figure 2.13** – Electric circuit analogous to measuring flow resistance.

This system is described by the following equations.

$$i_C = C \frac{dV}{dt} \quad (2.28)$$

$$i_R = \frac{V}{R} \quad (2.29)$$

$$i_R + i_C = I_0 \quad (2.30)$$

Hence a first order linear differential equation with corresponding solution is obtained.

$$C \frac{dV}{dt} + \frac{V}{R} - I_0 = 0 \quad (2.31)$$

$$V(t) = I_0 R (1 - \exp(-t/RC)) \quad (2.32)$$

It is to be expected that filling the capillaries (which will have a fluidic capacitance as the circuit used to transport the liquid from the source to the capillary can expand) will show similar behavior.

## 2.8 Modes

Up until now, only the mode in which a cone and jet occurs has been discussed. However, as described by Jaworek<sup>6</sup> several modes can occur (refer to Figure 2.14). These modes can be grouped into two major categories: *dripping* modes, in which droplets are ejected from the tip directly and *jet* modes, in which first a long and thin jet arises whereupon droplets are created. However, the cone-jet mode is the most important and widely used one (refer to e.g. Smith,<sup>10</sup> Kebarle,<sup>9</sup> de la Mora<sup>18</sup>).

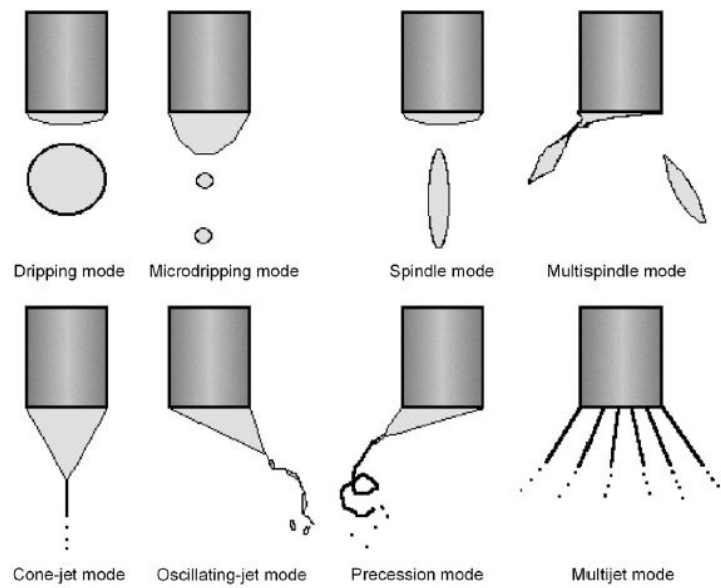


**Figure 2.14** – Overview of modes. The upper four modes are *dripping* modes whilst the lower four show *jet* modes. The cone-jet mode (lower most left) will be discussed in this study. Adopted from Jaworek.<sup>6</sup>

# Chapter 3

## Method

### 3.1 Electrospray setup

In order to carry out the electrospray measurements a setup has to be constructed. Several design requirements have to be taken into account:

- Especially the counter electrode, but also the capillary (mounted to a syringe) has to be isolated electrically from the rest of the setup
- The whole setup has to be viewed easily by a microscope
- The tip-electrode distance has to be adjusted easily and accurately
- It must be possible to *measure* the tip-electrode precisely
- It must be possible to change the syringe, capillary and counter electrode relatively easily without modifying the entire setup
- The setup has to be safe while working with very high voltages
- Environmental parameters like ambient temperature, humidity and air composition should have minimum influence on the process

Taking this points into account and lots of trial and error resulted in a setup (see Figure 3.1 and Figure 3.3).

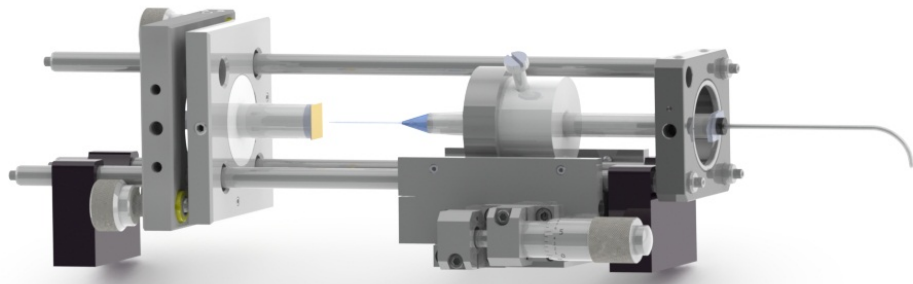


**Figure 3.1** – The electro spray setup. For convenience in this figure the setup has been flipped 90 degrees over the long axis (see Figure 3.2).



**Figure 3.2** – Actual orientation with microscope eyepiece.

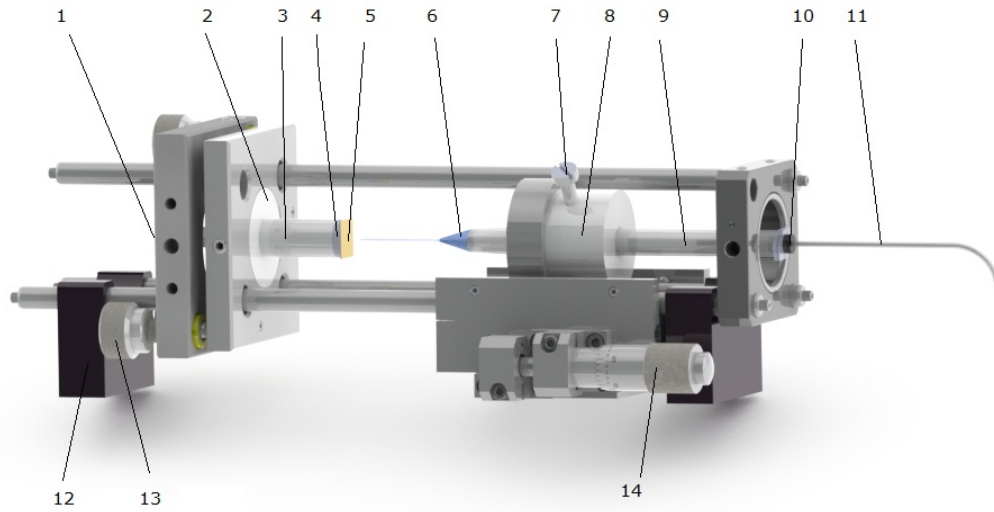


**Figure 3.3** – The most important parts of the setup have been indicated by numbers. Note that this figure has also still been flipped 90 degrees over the long axis.

First, a stainless steel nail shaped counter electrode (4) has been mounted in a macor cylinder (3), which is, in turn, mounted in a teflon cylinder (2). These materials isolate the counter electrode electrically from the rest of the setup. This whole unit is fixed in a frame that can be translated using the translator (13). The - pole of the source is connected to the setup at (1). Triax cables are used for connections between the setup and the source measurement unit. These cables are both safe and reduce the capacitive function of the setup. The source measurement unit (Keithley 237 high voltage SMU) is able to measure I-V curves and set a compliance to the current. The process is visualized using a Mitutoyo FS-70 microscope with eyepieces with 10, 20 and 50 times magnification. A silicon wafer with a gold layer (5) has been glued to the counter electrode using silver glue. The capillary is mounted to an 1 ml syringe (9). A very tiny hole is drilled in the syringe. Through this hole a thin platinum wire is fixed (6). The + pole of the source is connected to this wire. The syringe is located inside a teflon cylinder (8) which can be fixed using a nylon nail (7). Next 1/16" tubing (11) is connected to the syringe using a plunger (10). The liquid from a pressure vessel will enter the setup here. The capillary distance can be adjusted very accurately using the translator (14). The whole setup is mounted to the microscope frame using two holders (12).

The syringe is the element which is touched most frequently so it's safe to have this a 0V. In order to maintain a potential drop from capillary to counter electrode a voltage of e.g. -800 V is applied to the counter electrode.

In addition, all metal parts except the counter electrode have been grounded to provide maximum safety.

Even though the use of triax cables decreases the RC time of the system significantly, it is to be expected that the setup has a certain nonzero RC time (also ordinary copper wires had to be used sometimes). This has to be taken into account during the measurements: it can take some time before the current is more or less constant.

### **3.1.1 Tip-electrode distance**

In order to determine the tip-electrode distance the reflection of the capillary in the counter electrode is used. The distance between the tip and reflected tip is (ideally) two times the tip-electrode distance. This method also reduces the measurement error by a factor 2.

Stainless steel is, however, quite dull so the reflection is hard to see. Initially a silicon wafer was used to solve this problem. A wafer is very flat so the tip-electrode distance does not change if the capillary goes up  $1\mu\text{m}$  for example. However, an oxide layer grows on a silicon wafer in an aerobic environment which makes it non-conductive. Therefore a silicon wafer with a gold layer is mounted to the counter electrode (refer to Figure 3.5). This is connected electrically using silver glue.

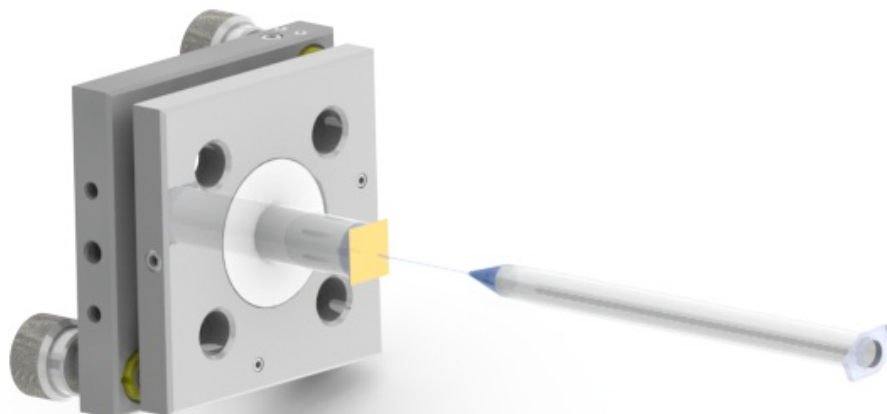


**Figure 3.4** – A closeup of the syringe and counter electrode. The gold layer reflects much better than stainless steel.

The tip-electrode distance can be measured accurately, but it is hard to tune the distance with microns. So it is possible to set the tip-electrode distance at e.g.  $31 \mu\text{m}$  and measure it accurately, but it is hard to change this distance into  $30 \mu\text{m}$ . The distance can be measured real time.

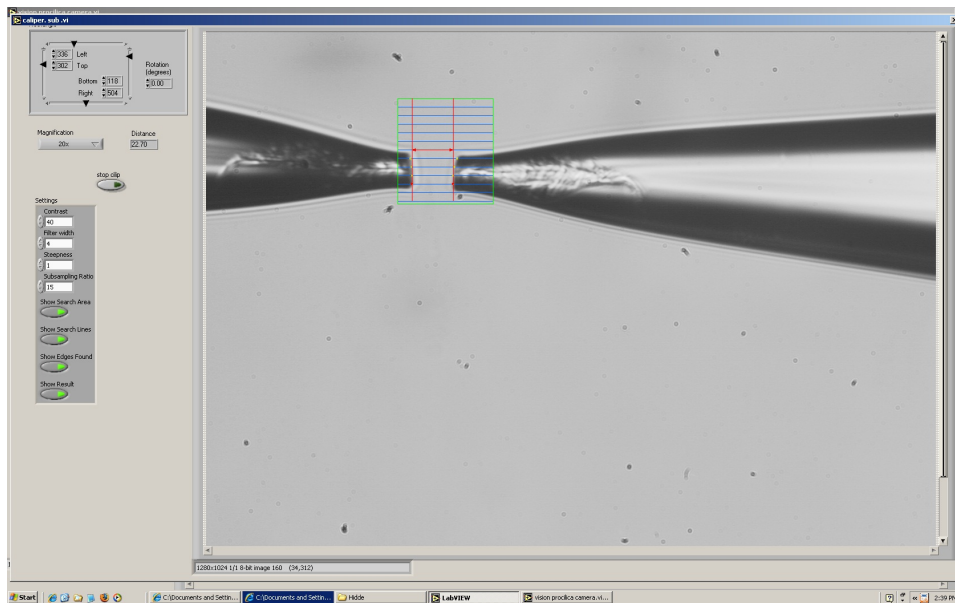


**Figure 3.5** – LabView software is able to measure the tip-tip distance (so twice the tip-electrode distance) real time which makes it easy to set the right distance.

### 3.1.2 Angular rotations

The golden layered wafer has been placed on the counter electrode to see the reflection of the tip and therefore being able to determine the tip-electrode distance. However, if the wafer is entirely normal to the eyepiece of the microscope nothing can be seen. Therefore the setup has to be put under a small angle (see Figure 3.6).

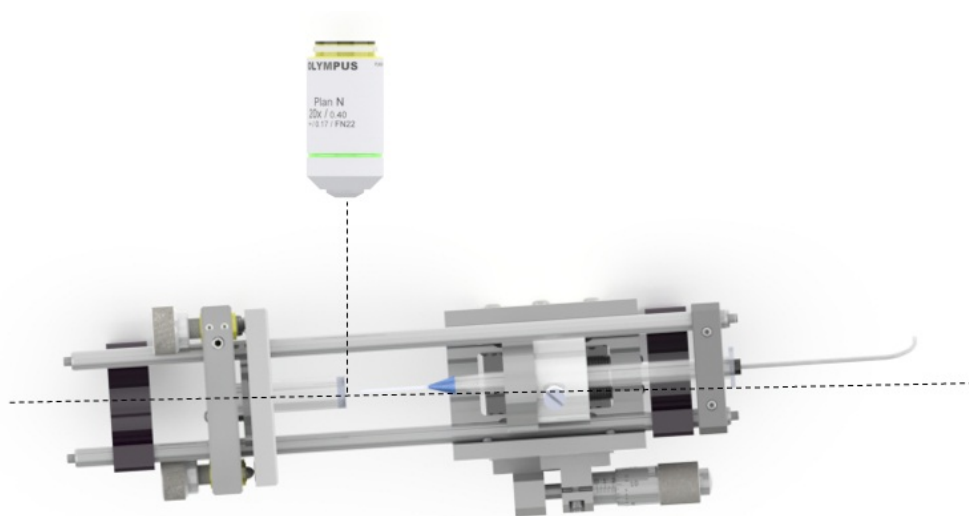


**Figure 3.6** – The setup has been rotated with respect to the eyepiece of the microscope.

As long as the capillary is exactly normal to the wafer no turning in the mirror can be observed; this is more or less the definition of a mirror (refer to Figure 3.7).

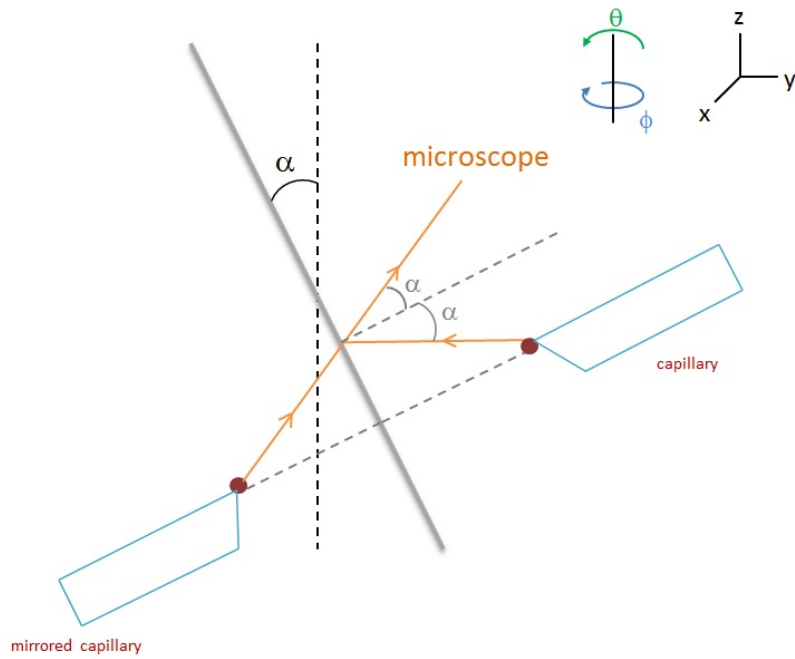


**Figure 3.7** – Reflection of a capillary entirely normal to the wafer. For the sake of clarification the capillary has not been drawn symmetrically intentionally.

However, the capillary will never be exactly normal to the wafer. The capillary itself is quite straight, but the lock to the syringe and the cylinder in which the syringe is locked are not. This causes a rotation in the mirrored capillary which gives a distorted reflection (refer to Figure 3.8).

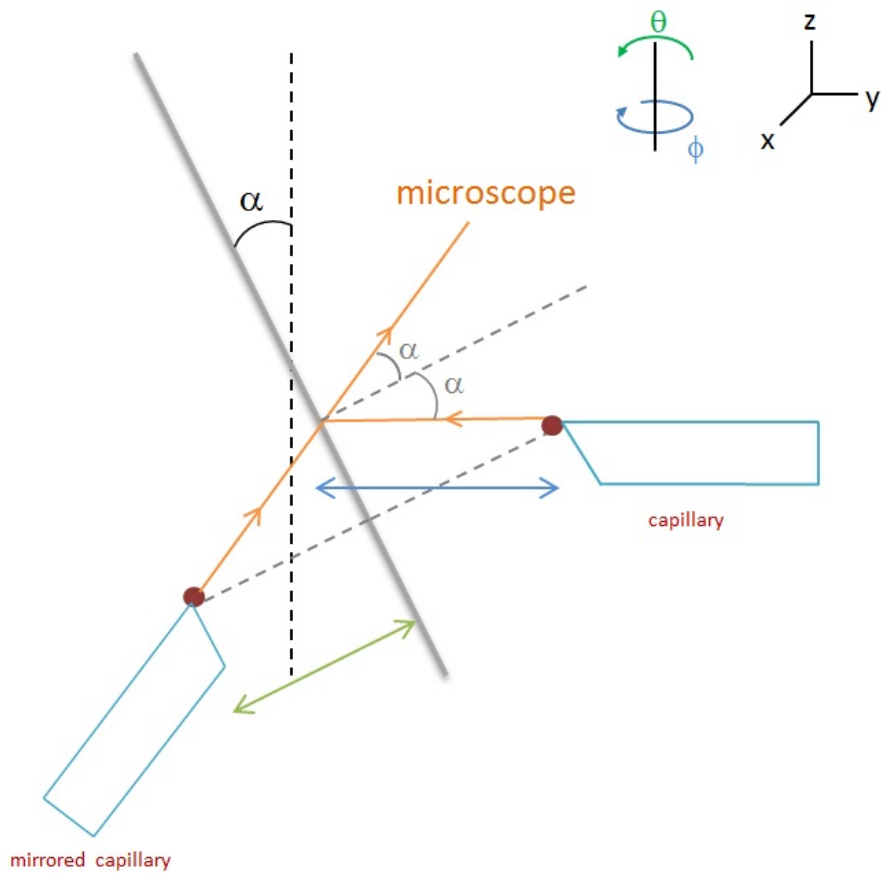


**Figure 3.8** – Here the capillary is not normal to the wafer. In the microscope the (true) wafer-tip distance (indicated by the blue arrow) can be seen. However, the wafer-mirrored tip distance is indicated by the green arrow. This distance is reduced with respect to the actual distance. Note this drawing only describes the rotation in  $\theta$  direction, but this also holds for the  $\phi$  direction.



**Figure 3.9** – A  $10\mu\text{m}$  capillary 10x magnified. It can be observed that the mirrored capillary on the left is slightly rotated with respect to the capillary on the right. Note that this may seem like a huge rotation, but the capillaries are made of glass so they are translucent. This makes it hard to see the actual opening. In addition, the mirrored capillary has been rotated in both  $\theta$  and  $\phi$  direction.

If, for the sake of simplicity, the capillary is assumed to be parallel to the ground (i.e. perpendicular to the black dashed line) the actual wafer-tip distance  $d_a$  (blue arrow) and the mirrored wafer-tip distance  $d_m$  (green arrow) can be related as:

$$d_m = d_a \cdot \cos(\alpha) \quad (3.1)$$

So it seems there is a closed relation between the two distances hence the actual wafer-tip distance should be easy to determine. However, the angle  $\alpha$  is very hard, if not impossible, to determine. It is possible to make an estimation of the angle. If the angle is stated to be small a Taylor expansion can be performed:

$$\cos(\alpha) = 1 - \frac{\alpha^2}{2} + O(\alpha^4) \quad (3.2)$$

For small values of  $\alpha$  the squared term is approximately zero. This makes sure the mirrored and actual tip-wafer distance are more or less equal.

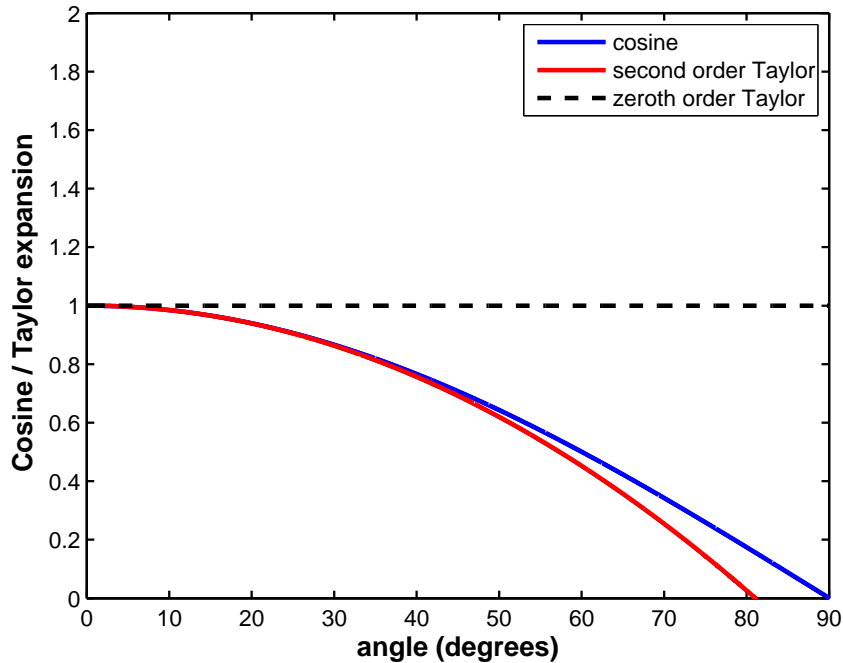


**Figure 3.10** – The Taylor approximations compared to the actual cosine function. If the angle does not exceed 20 degrees the error will be 6 percent at max. This is an acceptable mistake.

### 3.1.3 Filling and filtering

Filling the capillaries can become quite cumbersome. The capillary action causes the capillary to suck, but this force is not big enough to pull the plunger of the syringe. Therefore a pressure system has been developed. Nitrogen at a pressure of about 1.5 bar is led into a pressure vessel which contains the spraying liquid. A very precise pressure regulator is used to fill the capillary. The liquid from the pressure vessel is pushed through an in-line filter with  $0.2 \mu\text{m}$  pores using an  $1/16$  inch tube. For the  $10 \mu\text{m}$  capillaries a  $2 \mu\text{m}$  filter has been used. If this filter is not used dirt (particles) will clog the capillaries as the channels are very thin and fragile.

Because this filter causes quite a pressure drop and the pressure applied to the capillary is an important parameter to know a pressure sensor (Honeywell 26PC C type, scope of 0-1 bar) is placed between the syringe and filter.

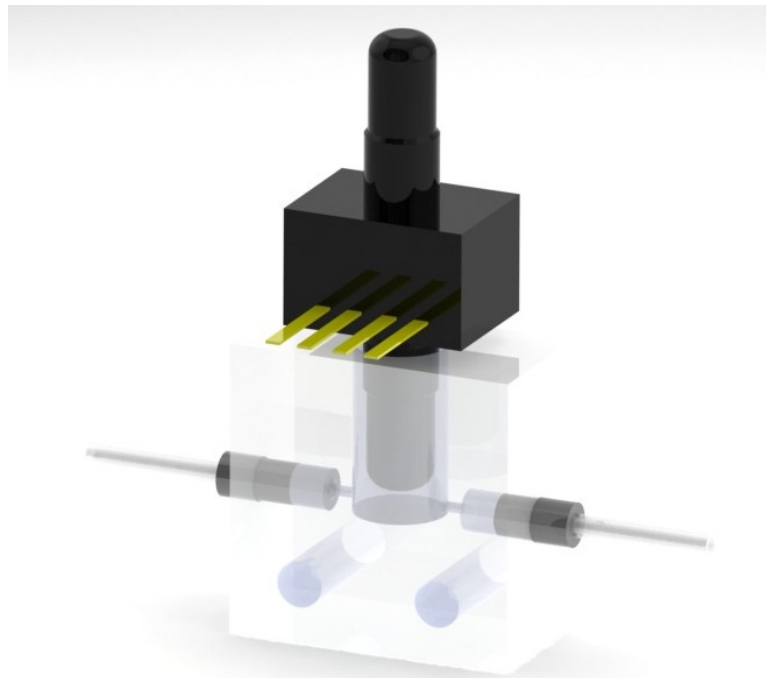


**Figure 3.11** – The pressure sensor is connected using 1/16 inch tubing.



**Figure 3.12** – Representation of the syringe, capillary and pressure sensor free from the setup. The filter is placed in front of the pressure sensor in order the measure the actual pressure applied to the capillary.

The pressure sensor gives a linear relation between the indicated voltage and actual pressure. The sensitivity curve has been plotted in Figure 3.13.

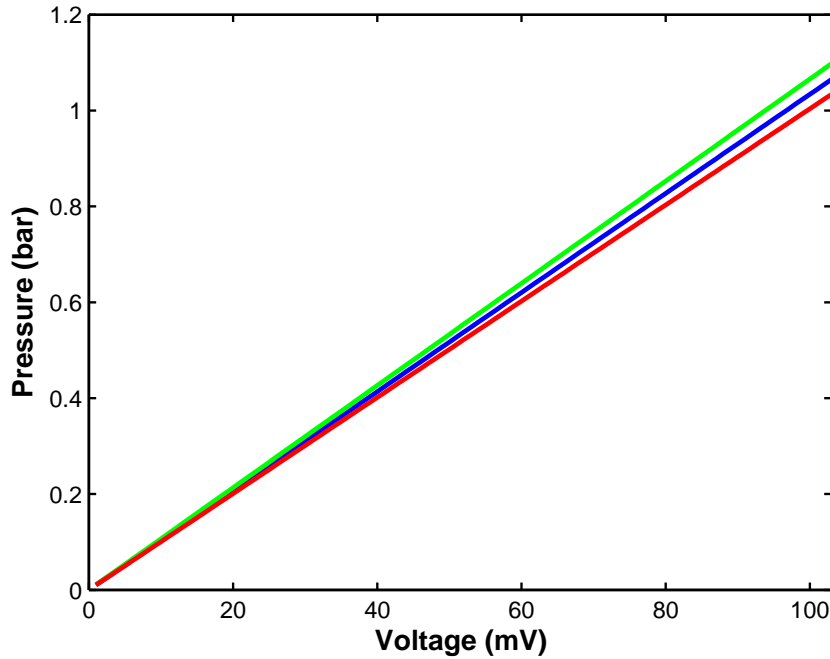


**Figure 3.13** – Note this pressure is the excess pressure with respect to the ambient pressure ( $p_0$ ). The green line gives the maximum, the red line the minimum and the blue line the typical value.

### Filling time

10  $\mu\text{m}$ , 1  $\mu\text{m}$  and 100 nm capillaries (World Precision Instruments) are used. Because they have been pulled no precise information about their dimensions, other than the tip radius, is known. However, using Equation 2.27 the time needed to fill the capillary can be estimated. The capillaries do not have the same small diameter everywhere. A schematic representation is given in Figure 3.14.



**Figure 3.14** – For the  $1\mu\text{m}$  and  $100\text{ nm}$  capillaries the inner diameter of course reads respectively  $1\mu\text{m}$  and  $100\text{ nm}$  and not  $10\mu\text{m}$ . The inner diameter is represented by the dashed black line. The Luer lock is indicated by the thick blue lines and the syringe by the red lines. So the parts that play a role in the time of the filling process are black in this figure.

Using Equation 2.27 it can be stated that:

$$Q = \frac{\Delta p}{R_V} = \frac{\Delta p \cdot \pi r^4}{8\mu L} \quad (3.3)$$

The system, however, has a capillary, tubing, syringe etc. that are not perfectly symmetrical. The system's resistance can be estimated by taking ideal tubes with fixed diameter in series. An expression for  $Q$  is obtained:

$$Q = \frac{\Delta p \cdot \pi}{8\mu} \sum_i \frac{r_i^4}{L_i} \quad (3.4)$$

However, the flow rate is not the most interesting parameter, but the time it takes to fill a certain volume  $V$  is. Flow rate  $Q$  is defined as

$$Q \equiv \frac{dV}{dt} \quad (3.5)$$

If  $V$  depends linearly on time and we take 0 time and volume as reference this yields

$$Q = \frac{V}{t} \Rightarrow t = \frac{V}{Q} \quad (3.6)$$

Hence the filling time  $t$  can be described as

$$t = \frac{8\mu V}{\Delta p \cdot \pi} \sum_i \frac{L_i}{r_i^4} \quad (3.7)$$

However, the radius of the syringe, tubing, wide part of the capillary etc. is about 50 times the tip radius (or even more). As the filling time decays with  $1/r^4$  these terms are all negligible. So the only term that matters in the flow resistance is the capillary tip. However, the complete capillary has to be filled so the 42 mm with 0.5 mm diameter has to be taken into account when calculating the volume to be filled. Taking  $\mu_{\text{air}} \approx 1.488 \cdot 10^{-5}$  P s a feeling for the order of the filling time (hours, days, years) can be estimated.

$$t \approx \frac{10^{-15}}{\Delta p \cdot r^4} \quad (3.8)$$

A pressure of  $0.05 \cdot 10^5$  Pa is a pressure at which the syringe is just dripping if the capillary is not mounted to it. If we take this pressure for  $\Delta p$  the time needed to fill the 10  $\mu\text{m}$ , 1  $\mu\text{m}$  and 100 nm reads respectively (the order is given between parentheses):

$$t_{10} \approx 20s \text{ (1 min)} \quad (3.9)$$

$$t_1 \approx 2 \cdot 10^5 s \text{ (2 days)} \quad (3.10)$$

$$t_{0.1} \approx 2 \cdot 10^9 s \text{ (years)} \quad (3.11)$$

Note that this time gives the absolute upper limit and therefore only a feeling for the order of size. In the approximation the peak of the capillary has been taken straight and not peak wise and the capillary action has not been taken into account at all. Taking both these phenomena into account will decrease the filling time significantly.

So the 10 $\mu\text{m}$  capillary can be filled real time and the 2 days of filling of the 1 $\mu\text{m}$  capillary can be done over the weekend which is acceptable. However, the 100 nm capillary could give problems.

### 3.1.4 Schematic representation

Taking all requirements into account the setup has been built. A schematic representation is given in Figure 3.15.

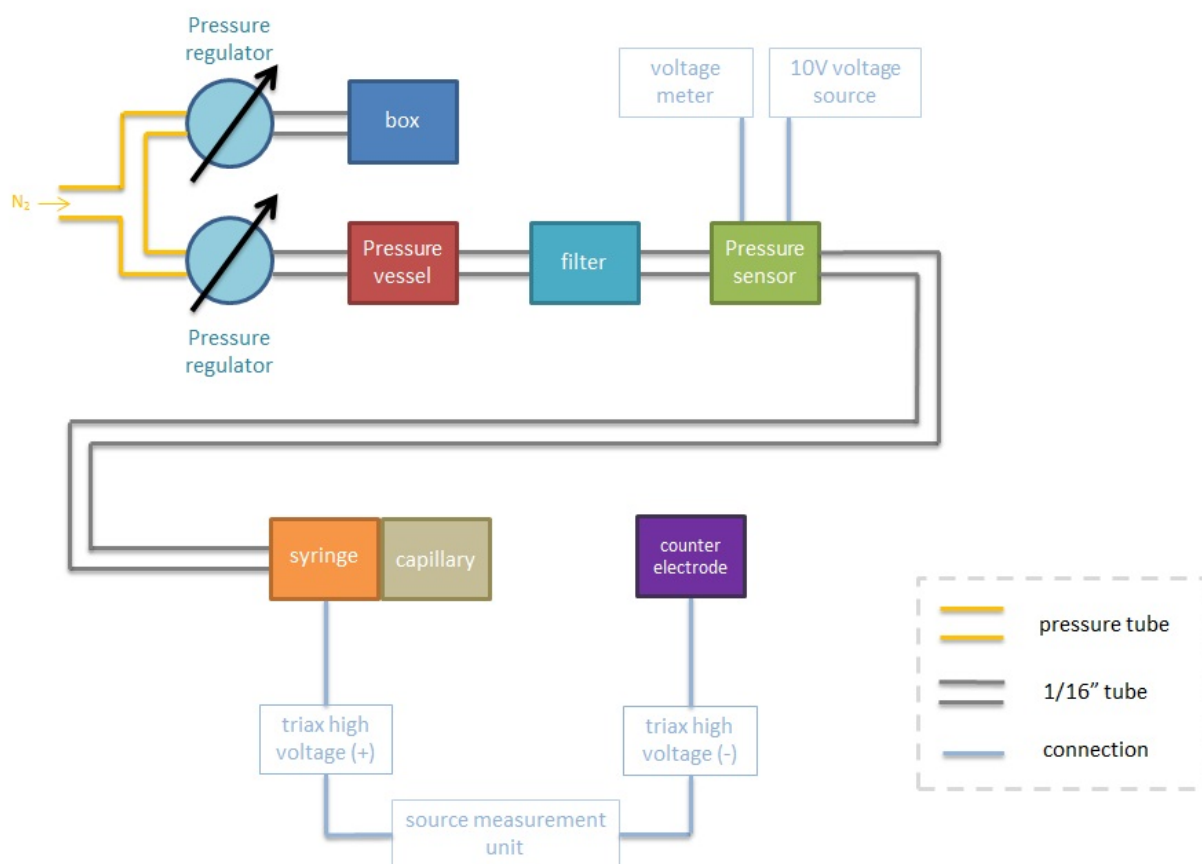


**Figure 3.15** – Schematic representation of the measurement setup. The nitrogen feed to the box makes sure the setup is surrounded with nitrogen having a lower humidity than ordinary air. This will bring down leaking currents.

## 3.2 Suitable liquids

The conductivity takes an important part in the electrospray process (refer to e.g. Equation 2.10 and Equation 2.21). Ideally, the liquid's conductivity is very high as described in subsection 2.5.1 and subsection 2.5.3. On the other hand, it is desirable that the same fluid has a low surface tension (as explained by Equation 2.4). These conditions do not go hand in hand so a compromise has to be reached.

The liquid's conductivity can be determined relatively easy using a conductivity meter (Mettler Toledo S40 SevenMulti pH/conductivity meter). The surface tension of a liquid is measurable, but it can be quite cumbersome. Therefore, (accurate) literature values have been used.<sup>34</sup>

In choosing the ideal liquid not only theoretical parameters like conductivity and surface tension are important. Also practical issues like availability and safety need to be taken into account. Very exotic substances can be used, but it's very convenient to work with non-hazardous fluids as (especially in the start up phase of the setup) it is hard to make everything hundred percent waterproof. If you use safe fluids it is not too bad if you spill something on your hands for instance. In addition, only few common used liquids are available in the lab. More exotic substances could have been ordered, but this would only establish an increase in conductivity of a couple of percent.

Taking this into account, a selection of possible liquids has been made. First, an acid is needed to increase the conductivity. Next, (de-ionized) water has to be added in order to let this acid do his work. Last, an alcohol can be added to decrease the surface tension of the substance. In Table 3.1 the surface tension for several alcohol/water mixtures is tabulated.

mass %	$\gamma$ (mN · m <sup>-1</sup> ), $T = 25^\circ C$			
	methanol/water	ethanol/water	1-propanol/water	2-propanol/water
0	72.01	72.01	72.01	72.01
5	62.77	55.73	41.83	49.58
10	56.18	47.53	34.32	40.42
15	51.17	42.08	30.36	34.63
20	47.21	37.97	27.84	30.57
25	43.78	35.51	26.64	28.28
30	41.09	32.98	25.98	26.82
40	36.51	30.16	25.26	25.27
50	32.86	27.96	24.80	24.26
60	29.83	26.23	24.49	23.51
70	27.48	25.01	24.08	22.68
80	25.51	23.82	23.86	22.14
90	23.93	22.72	23.59	21.69
100	22.51	21.82	23.28	21.22

**Table 3.1** – Surface tension of various alcohol/water mixtures. Note the mass % is given here, not the volume %. If the temperature is increased or decreased by 5 degrees, the surface tension will differ about 3 percent.<sup>34</sup>

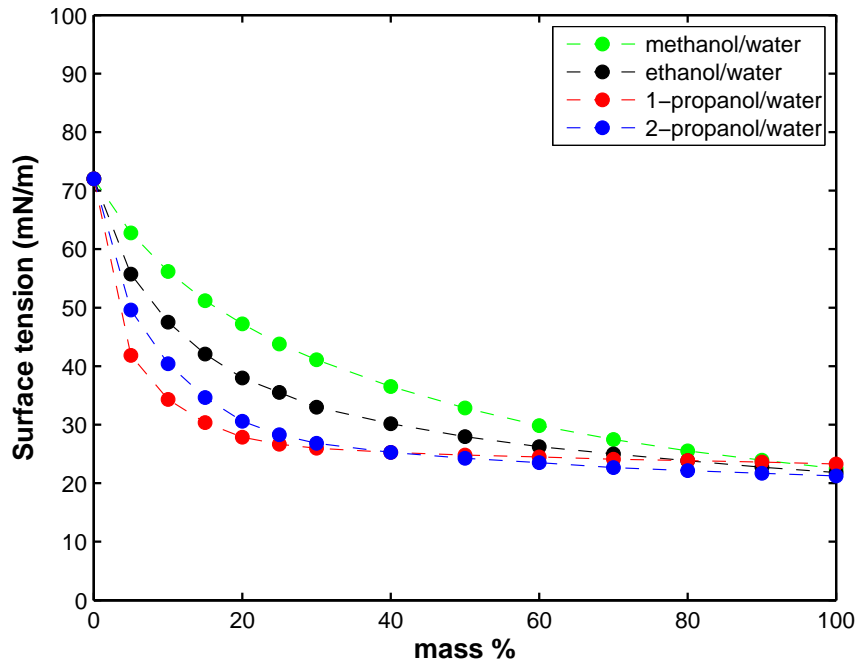


**Figure 3.16** – The exponential decay indicates the difference between the liquid’s surface tensions decreases if the alcohol/water fraction increases.

### 3.3 Flow resistance measurement

When applying pressure to a capillary both the Laplace pressure and the flow resistance of the system is 'felt'. As described in the previous chapter the Laplace pressure can be calculated quite accurately (refer to Equation 2.25). An expression for the flow resistance as a function of a tube’s length and radius has been derived (refer to Equation 2.26) as well. This expression is, however, only valid for a long and thin tube whereas the capillaries are tapered. In addition, the syringe in front of the capillary is not a perfect tube either.

In order to get a feeling for the flow resistance of the *total* setup the resistance can be measured analogous to measuring an electrical resistance. If a certain flow  $Q$  is applied and the pressure is measured the flow resistance can be calculated (according to Equation 2.26). In order to study only the flow resistance and not the resistance caused by the Laplace pressure the capillary has to be submerged in the same fluid as inside the capillary.

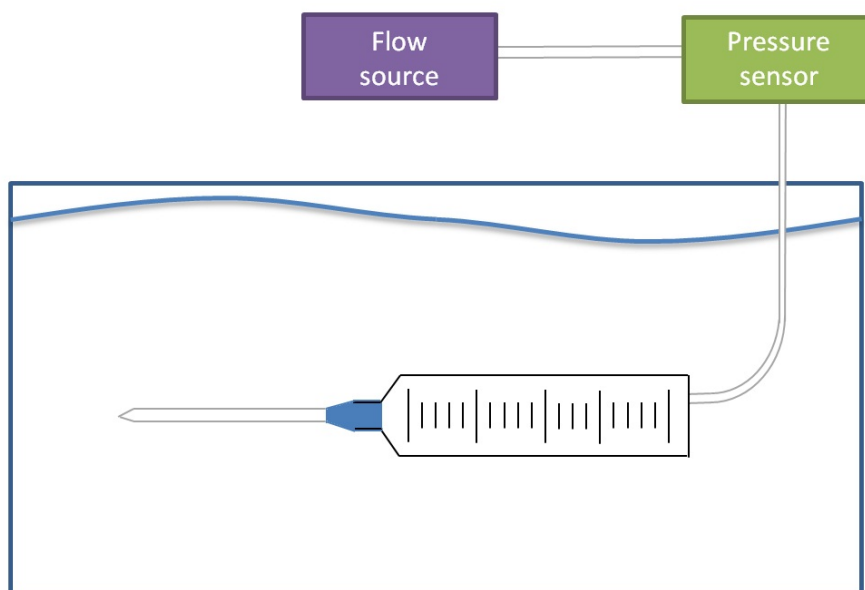


**Figure 3.17** – Schematic representation of the measurement setup.

As indicated schematically in Figure 3.17 a syringe pump (CMA 402 - flow rates from  $0.1 \mu\text{L} / \text{min}$  to  $20 \mu\text{L} / \text{min}$ ) in combination with an  $1.0 \text{ mL}$  syringe is used to generate a stable flow. The syringe is connected to the pressure sensor using  $1/16$  inch tubing. Next, the pressure sensor is connected to yet another  $1.0 \text{ mL}$  syringe (using the same tubing) on which the capillary is locked. Both the capillary and syringe are submerged in ultra pure DI water. The water pumped from the flow source into the capillary is the same ultra pure DI water, but this water has also been filtered using a filter with  $0.2 \mu\text{m}$  pores.

## Chapter 4

# Results

### 4.1 Flow resistance

Q ( $\mu\text{L min}^{-1}$ )	V <sub>sensor</sub> at Q=0 (mV)	V <sub>sensor</sub> ± 0.1 (mV)	p (bar)
5	0.5	2.2	0.0176
10	0.6	4.4	0.0393
15	0.6	6.3	0.0620
20	0.6	8.7	0.0838

**Table 4.1** – Measured values of pressure with various values of flow rate.

If no flow rate was applied, still some pressure was measured. This pressure is caused by the capillary forces and the fact that the system is closed. This pressure has to be taken into account as an offset. The results of Table 4.1 have been plotted in Figure 4.1.

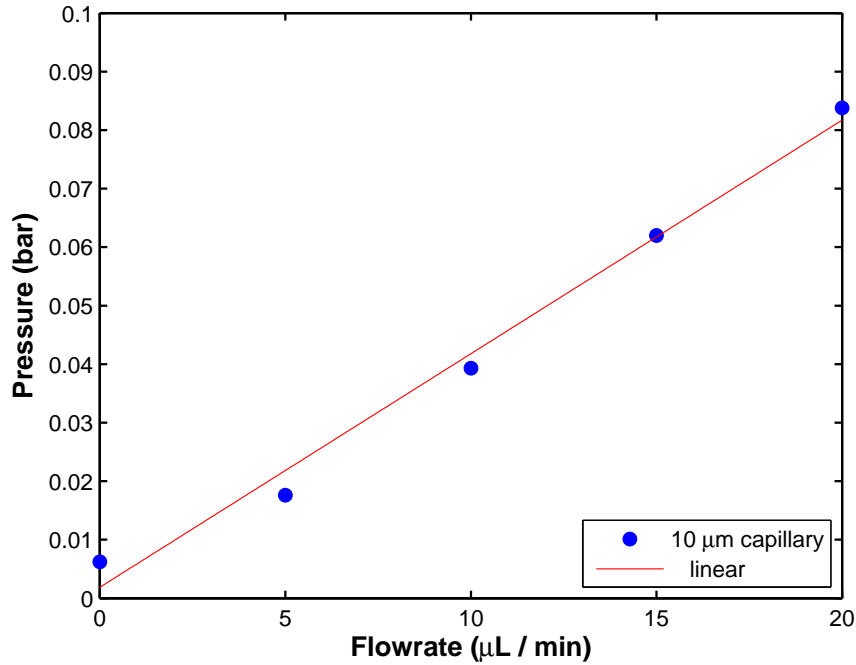


**Figure 4.1** – Pressure-flowrate diagram. The red line indicates the linear fit.

Equation 2.27 predicted a linear relation between flow rate and pressure in which the slope denotes the flow resistance. In Figure 4.1 a linear graph is drawn which follows the data points quite well. Determining the slope of the graph yields an expression for the flow resistance  $R_V$ :

$$R_V = 2.39 \cdot 10^{13} \text{ Pa s m}^{-3} \quad (4.1)$$

This result is very similar to the theoretical approximation (refer to Equation 2.26):

$$R_V = \frac{8\mu L}{\pi r^4} = \frac{8 \cdot 1.488 \cdot 10^{-5} \cdot 3.5 \cdot 10^{-3}}{\pi(10 \cdot 10^{-6})^4} = 1.33 \cdot 10^{13} \text{ Pa s m}^{-3} \quad (4.2)$$

Unlike a pure flow resistance it takes a certain time before a stable pressure is reached (refer to Figure 4.2).

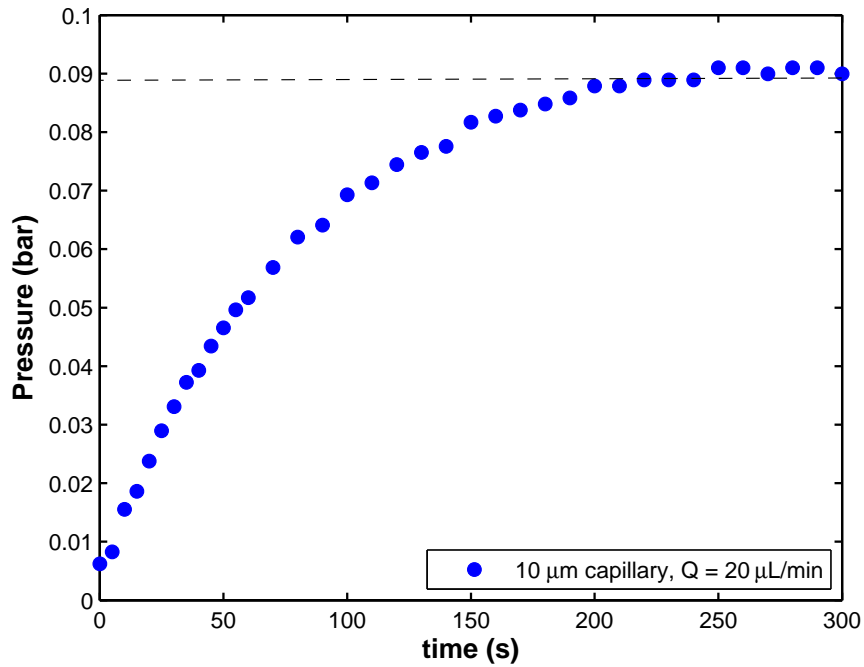


**Figure 4.2** – The pressure as a function of time behaves exponentially to a horizontal asymptote which is the stable pressure.

As described previously, this 'charging' phenomenon is completely analogous to the circuit in Figure 2.13. The capillary and tube do not only have a resistance, but also a certain fluidic capacitance. When the behavior of the electrical capacitor as described by Equation 2.32 is compared to the 'charging' of the capillaries great similarities can be observed (see Figure 4.3).

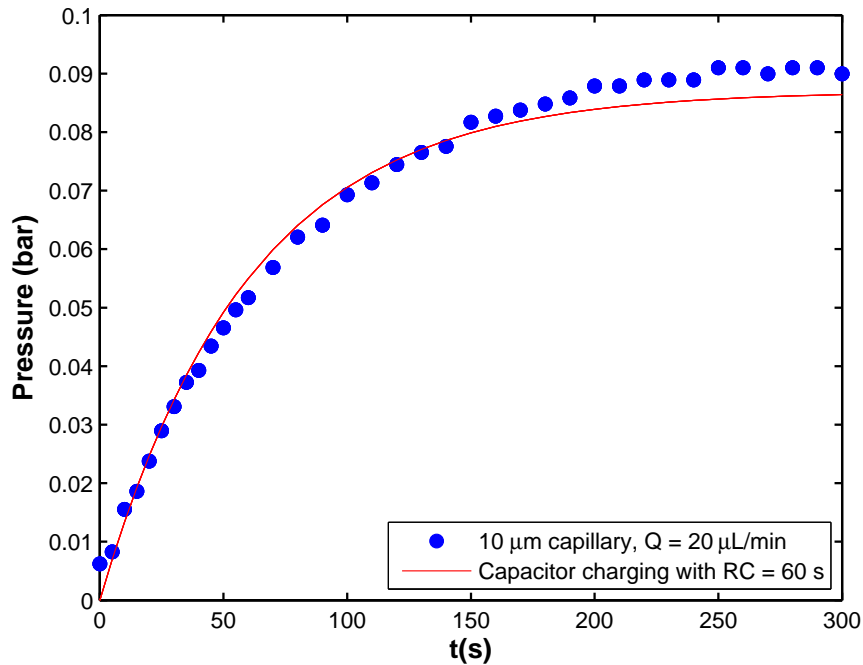


**Figure 4.3** – The red line indicates the charging behavior of a capacitance and resistor in series with an RC time of 60 s. This curves follows the fluidic date very accurately.

The RC-time is a value that gives an idea for the time it takes to charge a capacitor. After 3 times the RC time the capacitor is charged for 95%. Equation 2.26 predicts the resistance scales with  $1/r^4$ . So if the capillary is made 10 times smaller in radius (i.e. 1  $\mu\text{m}$  capillary) the resistance *increases* by a factor of 10.000. This resistance is not only not measurable by the used pressure sensor, the RC time is 10.000 times greater. Hence it lasts very long to obtain a stable pressure.

## 4.2 Counter electrode

It is important to know how the setup reacts to an applied voltage. In order to make sure no strange phenomena occur due to the counter electrode (because of bad connections for instance) the I-V characteristic of the counter electrode has been measured.

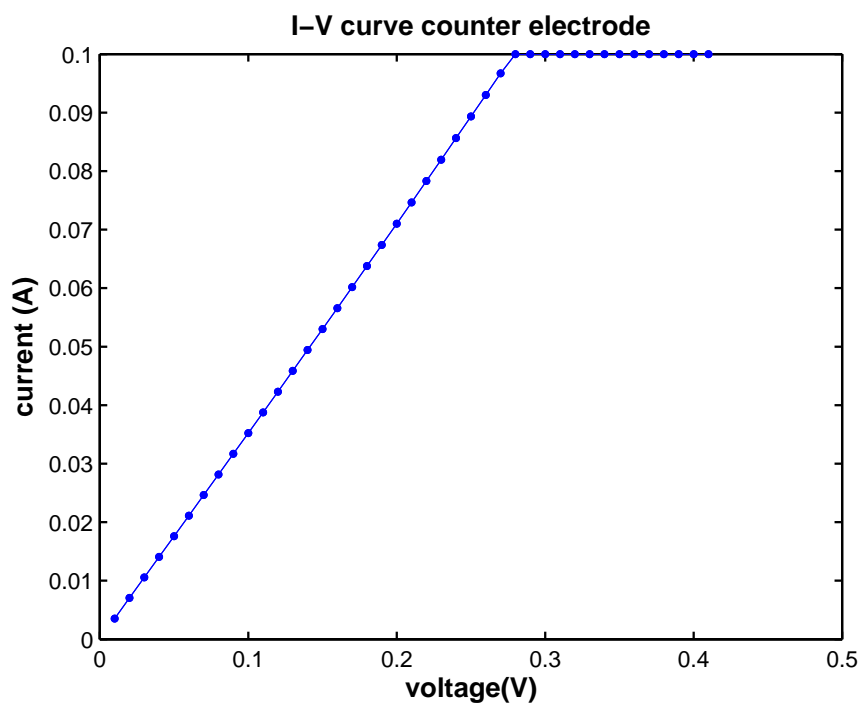


**Figure 4.4** – I-V curve of the counter electrode. Note the compliance is set at 0.1 A. So the current does not saturate at a certain voltage, but the source measurement unit limits the current to protect the setup. It can be observed that the counter electrode is virtually perfect Ohmic with a small resistance of about  $3 \Omega$ .

### 4.3 Conductivity measurement

In order to get a feeling for the conductivities of possible liquids various conductivities have been measured and plotted in Table 4.2.

liquid	$\gamma(\text{mN/m})^{35,34}$	$T(^{\circ}\text{C})$	$\sigma(\mu\text{S/cm})$
ethanol	22.3	20.7	5.85
acetic acid	27.6	21.1	16.82
ethanol (40%) / DI water	30.16	25.5	8.06
ethanol (80%) / DI water	23.82	22.6	12.02
acetic acid (80%) / DI water	$27.6 < \gamma < 40.6$	21.2	103.6
DI water	71.97	23.6	26.8
DI water with 12 g/L of salt dissolved	-	21.2	$38.2 \cdot 10^3$
ethanol (33%) / DI water (50%) acetic acid (17%)	$\gamma \approx 30$	20.6	790

**Table 4.2** – Conductivity of several liquids. The measurements were carried out at  $p = p_0$ .

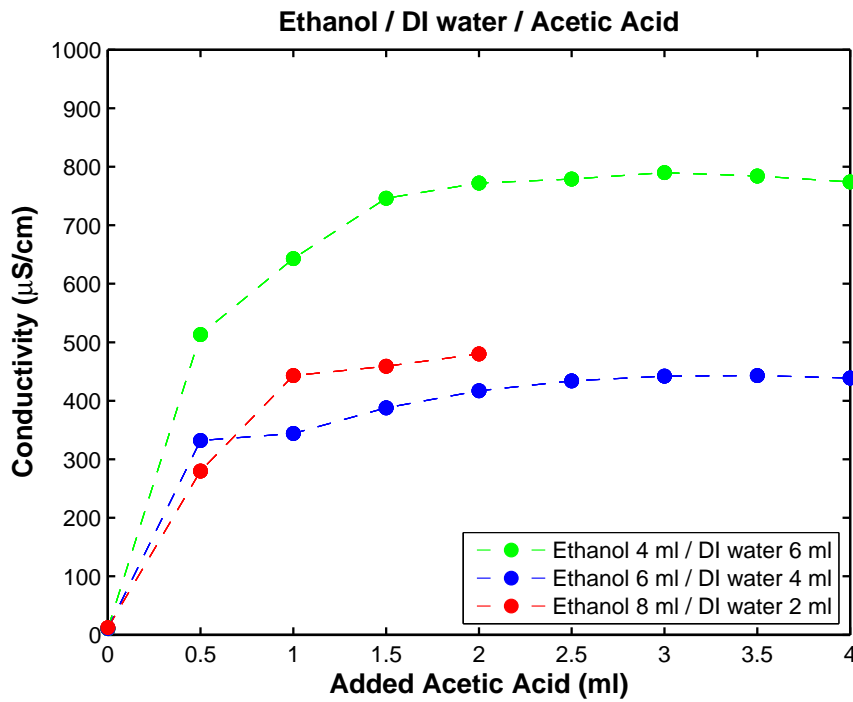


**Figure 4.5** – The conductivity does not increase linearly with the added acetic acid, but converges to a certain value. So adding more acetic acid will only *increase* the surface tension without increasing the conductivity.

It can be observed from Figure 4.5 that a solution of ethanol/DI water/acetic acid in the proportion 4:6:2 is the best compromise between high conductivity and low surface tension. This liquid will be used in the electrospray experiments, having a conductivity of  $790 \mu\text{S/cm}$  and a surface tension of

approximately 30 mN/m.

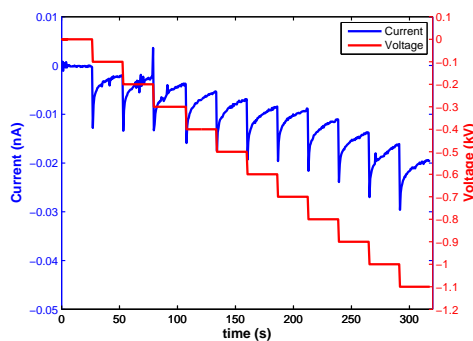
## 4.4 Electrospray

Before starting the actual electrospray measurements several reference measurements (i.e. obtaining I-V characteristics without liquid inside the capillary) have been carried out. From this leaking currents can be determined.

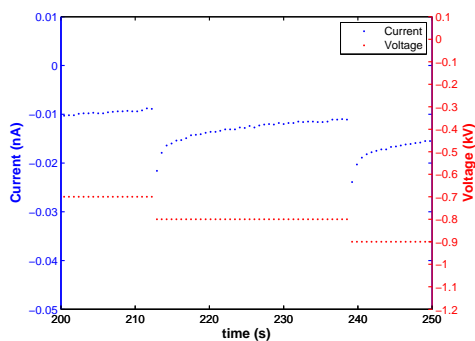
### 4.4.1 Reference measurements

#### 10 $\mu\text{m}$ capillary - air

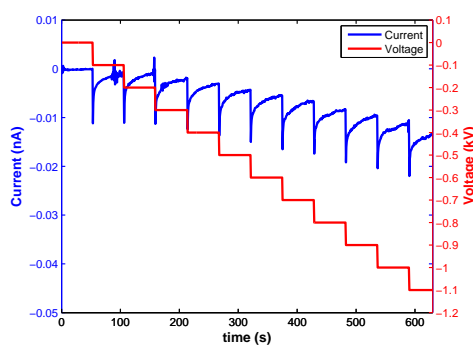
The measurements were performed at  $T = 21.5^\circ\text{C}$ ,  $p_{\text{amb}} = p_0$  and an environmental humidity of 42%.



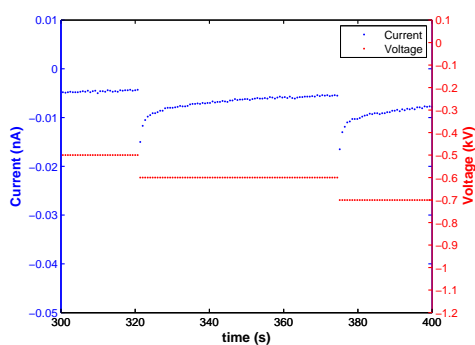
(a)  $d = 31 \mu\text{m}$ , 40 current measurements close up



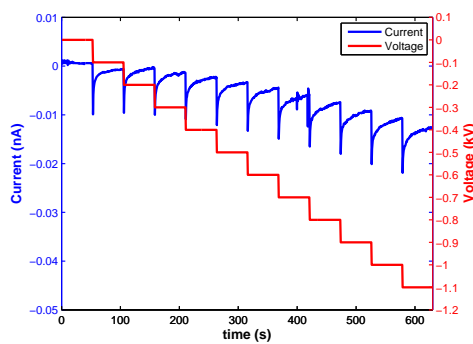
(b)  $d = 31 \mu\text{m}$ , 40 current measurements



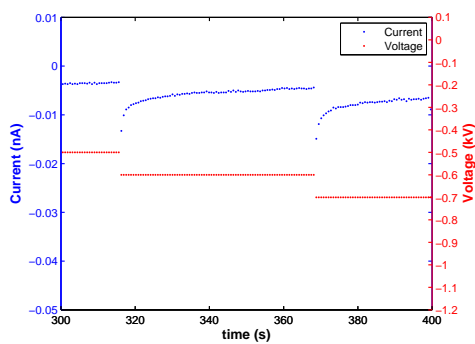
(c)  $d = 31 \mu\text{m}$ , 80 current measurements close up



(d)  $d = 31 \mu\text{m}$ , 80 current measurements



(e)  $d = 5 \mu\text{m}$ , 80 current measurements



(f)  $d = 5 \mu\text{m}$ , 80 current measurements closeup

**Figure 4.6** – Reference measurements for several tip-electrode distances. The red line indicates the steps in voltage whereas the blue line gives the current.

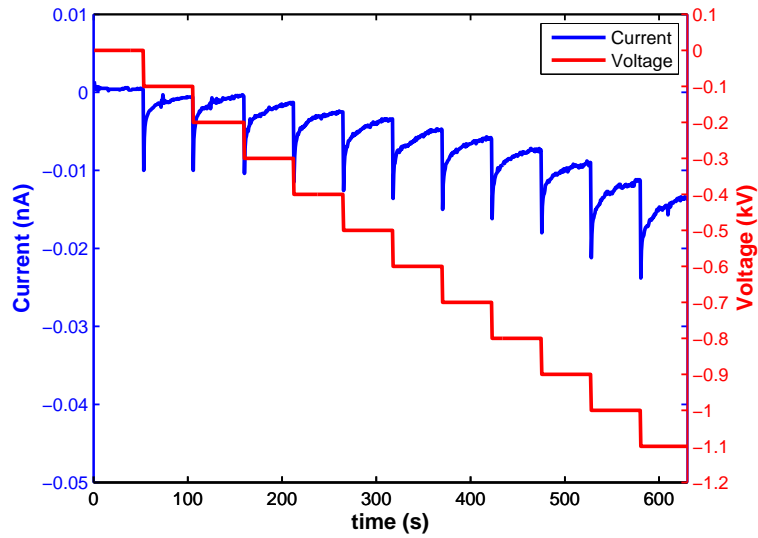


Figure 4.7 –  $d = 10 \mu\text{m}$  , 80 current measurements

### 10 $\mu\text{m}$ capillary - dry nitrogen

The measurements were performed at  $T = 21.5^\circ\text{C}$ ,  $p_{\text{amb}} = p_0$  and an environmental humidity of 25%.

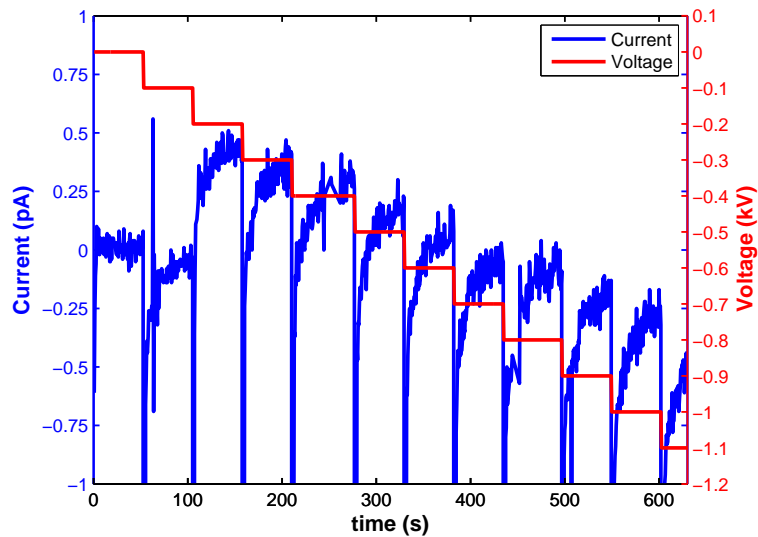
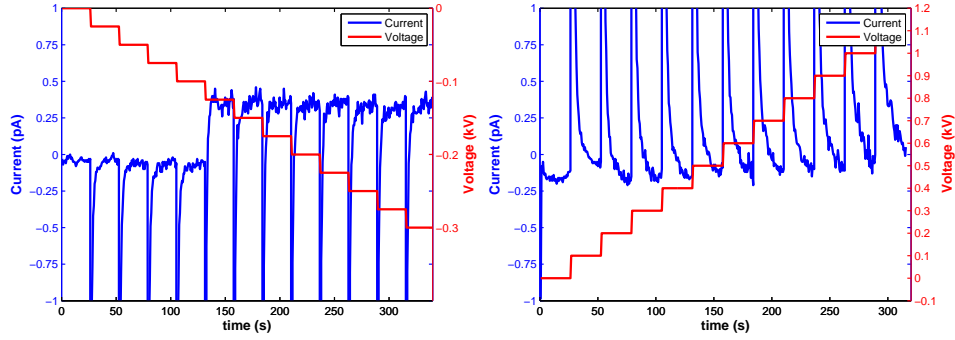


Figure 4.8 –  $d = 31 \mu\text{m}$  , 80 current measurements. Note the current is expressed in pA.

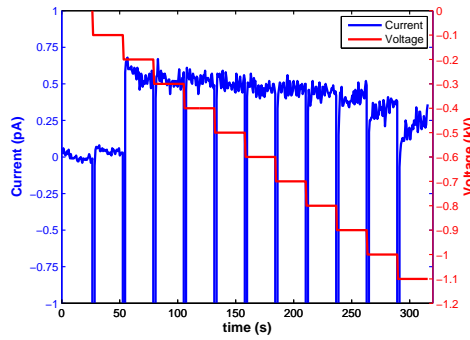
The step in current around 150 V can be characterized as remarkable. Sev-

eral other measurements have been performed to study this effect:



(a)  $d = 31 \mu\text{m}$ , 40 current measurements with a voltage step of 20V

(b)  $d = 31 \mu\text{m}$ , 40 current measurements, switched polarity of the voltage source



(c) No load

**Figure 4.9** – Reference measurements with smaller voltage steps (a), switched polarity (b) and no load at all (c).

It can be observed that the current step at approximately 160 V is also shown when no load at all is applied (i.e. nothing is connected to the source measurement unit). This makes it plausible this step is caused by the source measurement unit itself. However, the currents are very tiny (below 0.5 pA). So based on these reference measurements it can be stated that the leakage currents are approximately 500 times smaller than in the setup with air. They are smaller than 0.5 pA and therefore negligible. Further measurements will be performed in this 25% humidity environment rather than in air.

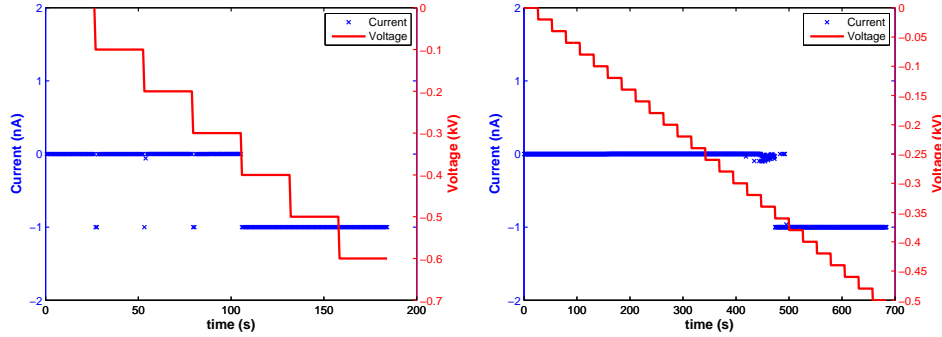
#### 4.4.2 Fluid measurements

For the electrospray measurements with liquid inside the capillary 36 ml of liquid has been prepared. This liquid consists of 18 ml ultra pure de-ionized water, 12 ml ethanol and 6 ml acetic acid. The liquid has a conductivity of  $790 \mu\text{S}/\text{cm}$  and a surface tension of approximately  $30 \text{ mN}/\text{m}$  ( $T=21.5^\circ\text{C}$ ). All measurements have been performed at a constant temperature of  $21.5^\circ\text{C}$ ,  $p_{\text{amb}} = p_0$  and in a dry nitrogen environment having a humidity of 25%.

Before studying the effects of pressure on the onset voltage several orienting measurements have been performed. Electrospray has also been performed using a relatively large needle of  $300 \mu\text{m}$  to visualize the process.

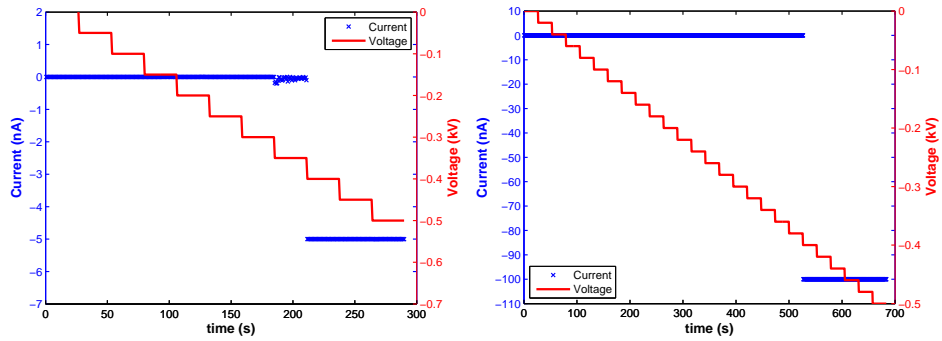
##### 10 $\mu\text{m}$ capillary

In order to fill the capillary a pressure of approximately 25 mbar has been applied. Note the various plots have various scales on the axes.



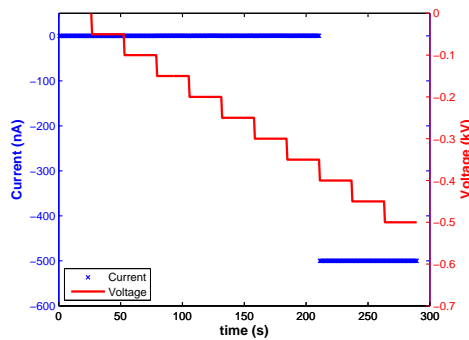
(a)  $d = 31 \mu\text{m}$ , compliance 1 nA, voltage step of 100V

(b)  $d = 31 \mu\text{m}$ , compliance 1 nA, voltage step of 20V



(c)  $d = 31 \mu\text{m}$ , compliance 5 nA, voltage step of 50V

(d)  $d = 31 \mu\text{m}$ , compliance 100 nA, voltage step of 20V

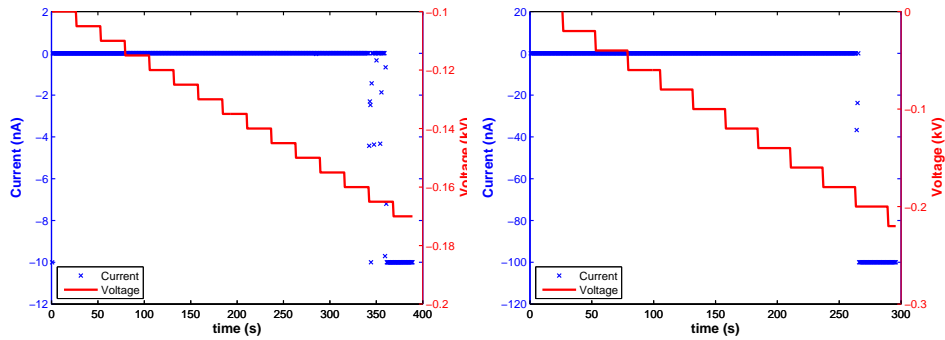


(e)  $d = 31 \mu\text{m}$ , compliance 500 nA, voltage step of 50V

**Figure 4.10** – Measurements for several voltage steps and compliances. Note that every time time the onset voltage (approximately 400V) is reached the current reaches the compliance almost immediately.

From the plots it can be seen that the onset voltage reads approximately

400 V.



(a)  $d = 9 \mu\text{m}$ , compliance 10 nA, voltage step of 5V

(b)  $d = 9 \mu\text{m}$ , compliance 100 nA, voltage step of 20V

**Figure 4.11** – Again, the compliance is reached almost immediately.

The onset voltage reads 165 V.

For both tip-electrode distances it is hard to study the current behavior as it reaches the compliance very fast (even if the compliance is set at 500 nA, which is a very high current). In addition, for high currents the liquid flow can become so large that the whole electrode is imbued with liquid creating a fluidic connection between capillary and electrode (refer to Figure 4.13).

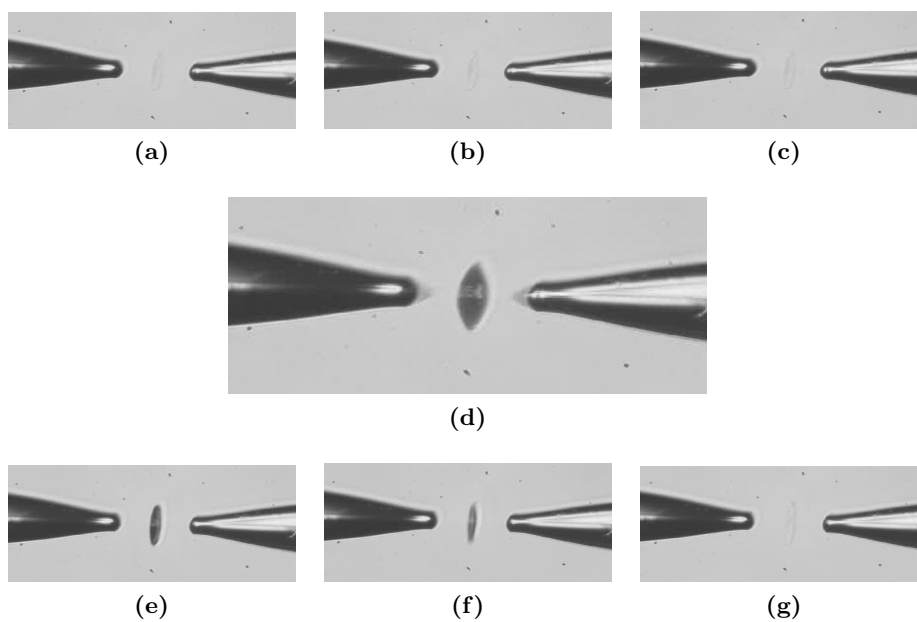


**Figure 4.12** – 20x magnification of the capillary at  $d = 31\mu\text{m}$ . The time increases from (a) to (g). At (d) the Taylor cone is visible. In addition, the liquid can be seen on the electrode in the middle of the capillaries at (d), (e) and (f). This proves there is electro-spray rather than just breakdown.

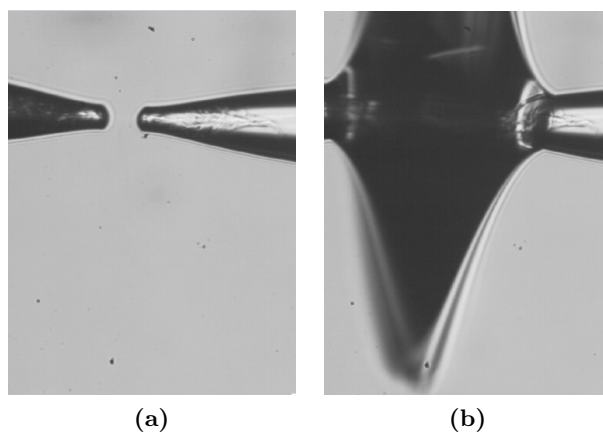


**Figure 4.13** – Example of a fluidic connection as a result of a too high compliance / flow rate. These captions were taken from a  $10\mu\text{m}$  capillary at  $10\mu\text{m}$  distance.

### 300 $\mu\text{m}$ needle

The measurements were performed at zero pressure.

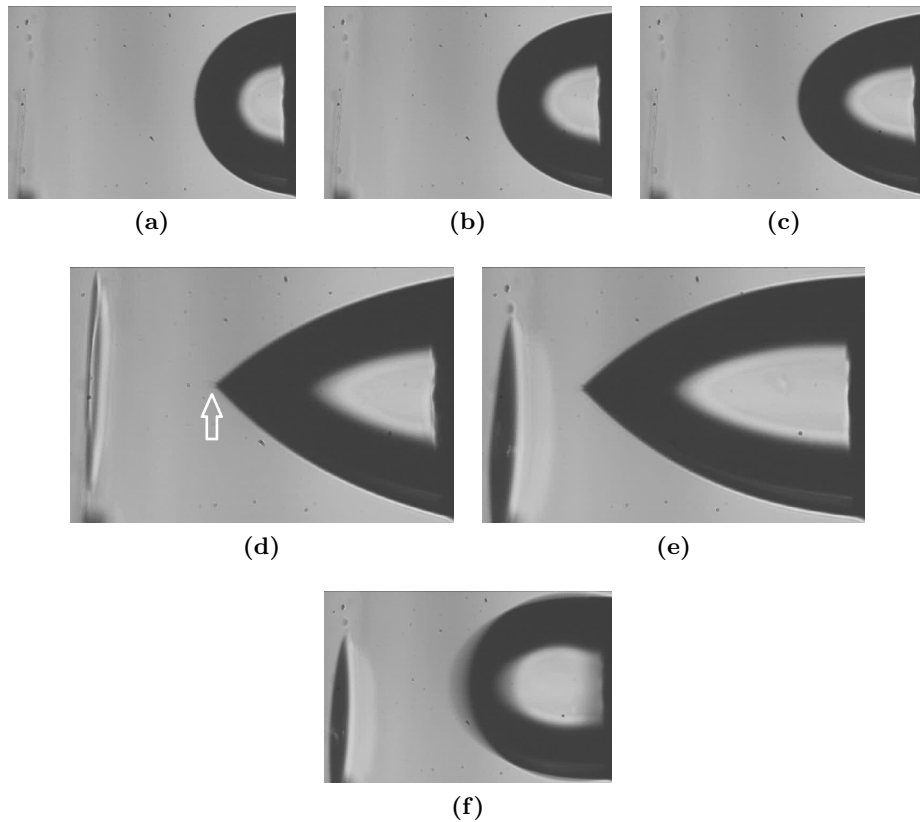


**Figure 4.14** – 10x magnification of the needle at  $d = 400\mu\text{m}$ . The meniscus is increasing with increasing pressure until the cone-jet mode at (d) is reached. The jet is indicated by the arrow in (d). Due to the compliance the cone-jet mode is not stable but pulsating; at (f) the Taylor cone pulls back again. From (d), (e) and (f) it can be observed that liquid reaches the counter electrode when the current hits the compliance which is, again, a proof that not just breakdown occurs.

#### 4.4.3 Fluid pressure measurements

The same liquid and parameters (temperature, ambient pressure and humidity) have been used. In all fluid measurements, unless stated, a compliance of 1 nA has been used. For every pressure - gap distance combination five measurements have been performed. For the sake of clarification only one measurement per combination has been presented in the following sections.

##### 10 $\mu\text{m}$ capillary - $d = 31\mu\text{m}$

In order to identify the range of the onset voltage first a large scope with a large voltage step has been applied.

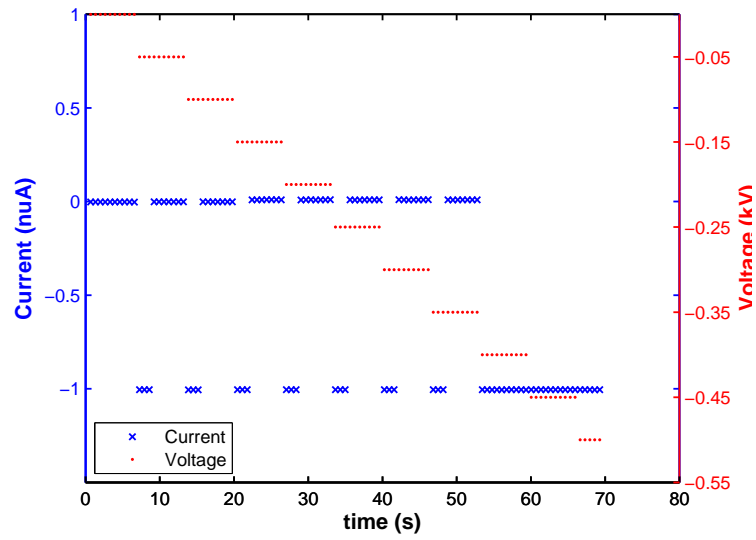


**Figure 4.15** – Voltage steps of 50 V are taken. It can be observed the onset voltage is in the order of 400V.

Knowing the order of onset voltage several more precise measurements at 0 - 50 mbar have been performed.

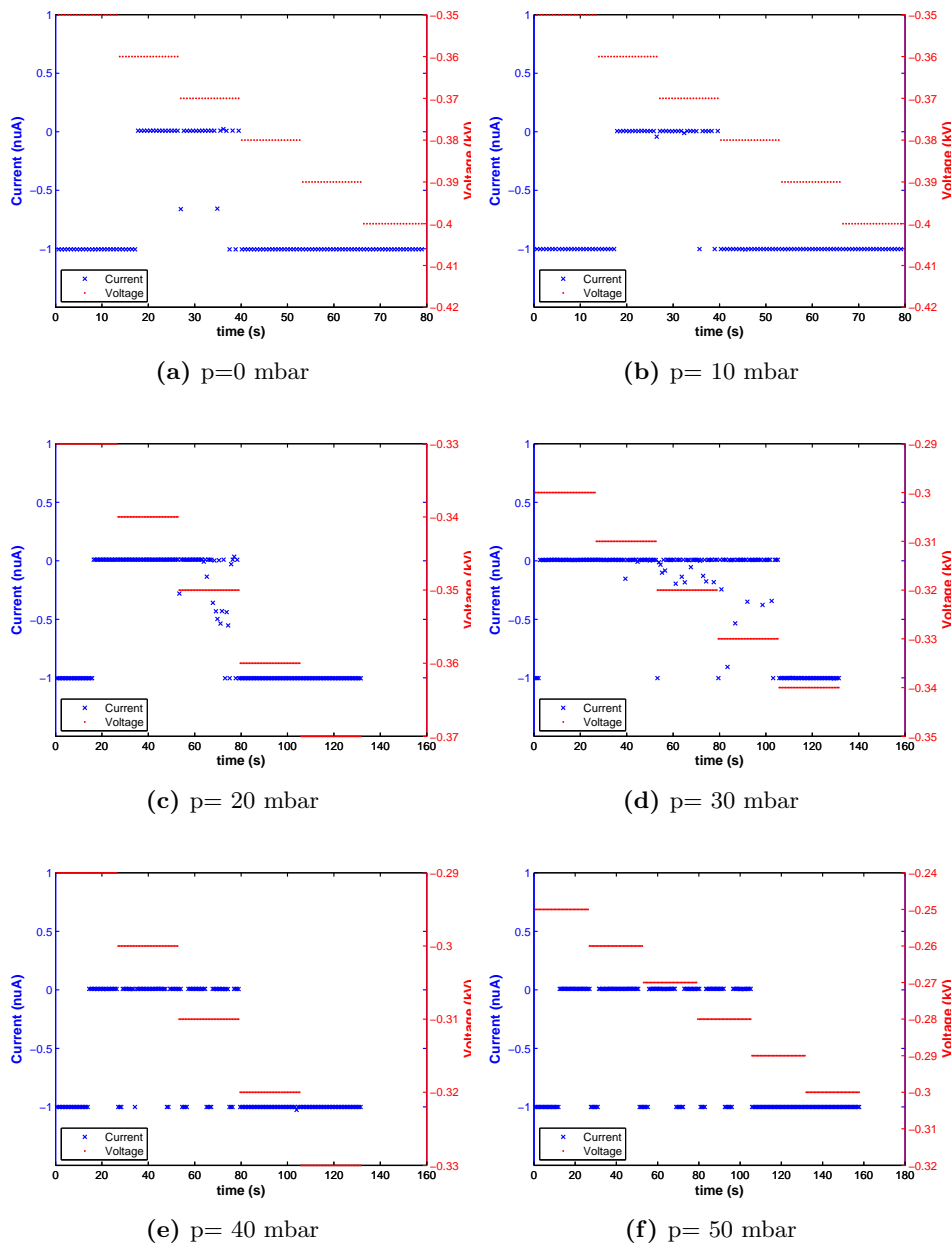


**Figure 4.16** – Measurements with voltage steps of 10 V at various pressures. The current at the beginning of the measurement is due to the large voltage step that is applied to the setup. The setup is slightly capacitive so applying a big voltage step will give a charging current. Therefore the the compliance of 1 nA is hit. It can be observed the onset voltage decreases with increasing pressure.

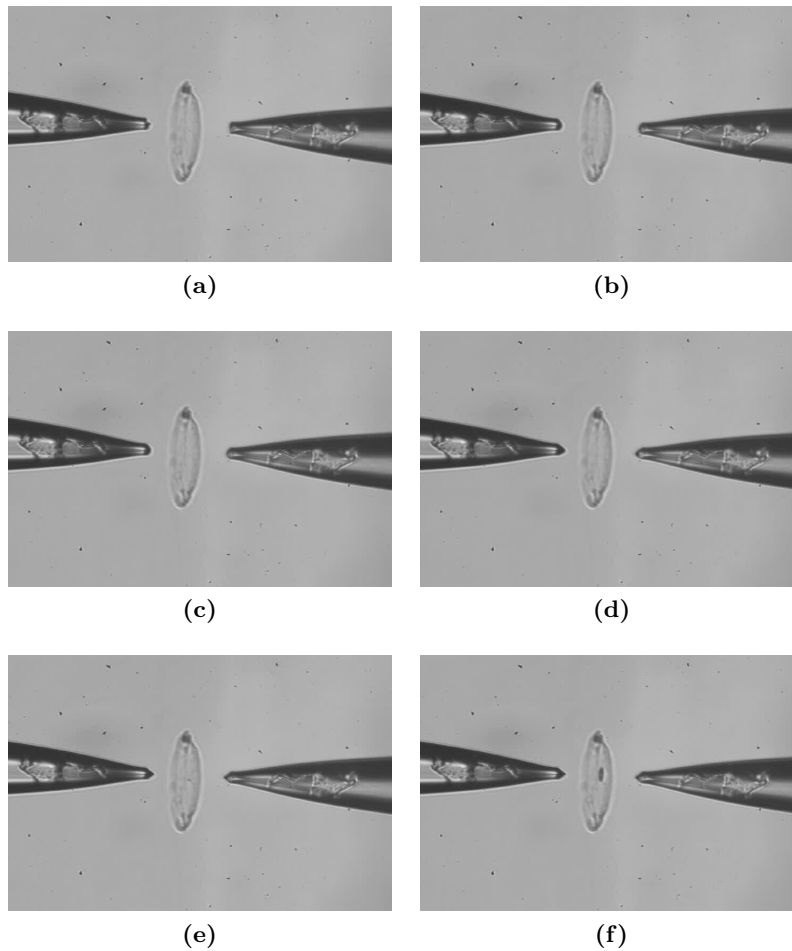


**Figure 4.17** – Captions of the spraying process. These figures are taken from the 0 mbar pressure measurement with a scope from 360 to 400V with increasing voltage from (a) to (f). The Taylor cone is clearly visible at (e) and the spraying can be observed at (f). The cone-jet mode is not stable, but pulsating.

**10  $\mu\text{m}$  capillary -  $d = 20\mu\text{m}$**

Again, in order to identify the range of the onset voltage first a large scope with a large voltage step has been applied.

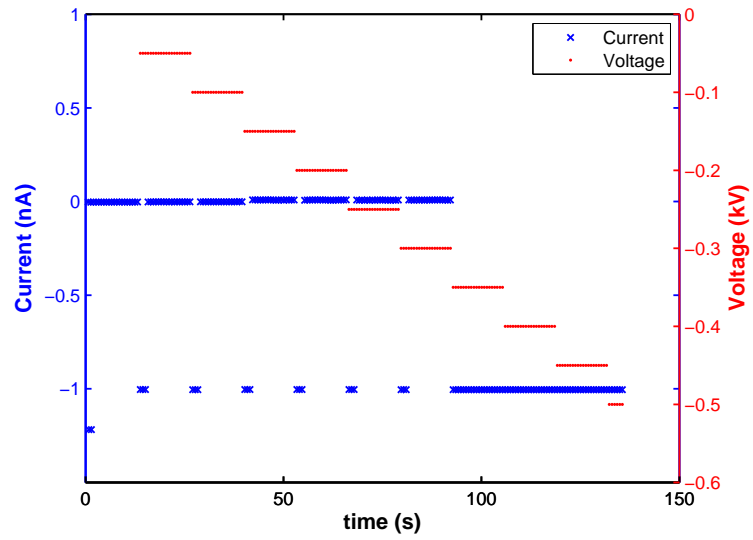


**Figure 4.18** – Voltage steps of 50 V are taken. It can be observed the onset voltage is in the order of 350V, which is lower than the 400V at  $d = 31\mu\text{m}$  which was to be expected.

Knowing the order of onset voltage several more precise measurements at 0 - 50 mbar have been performed.

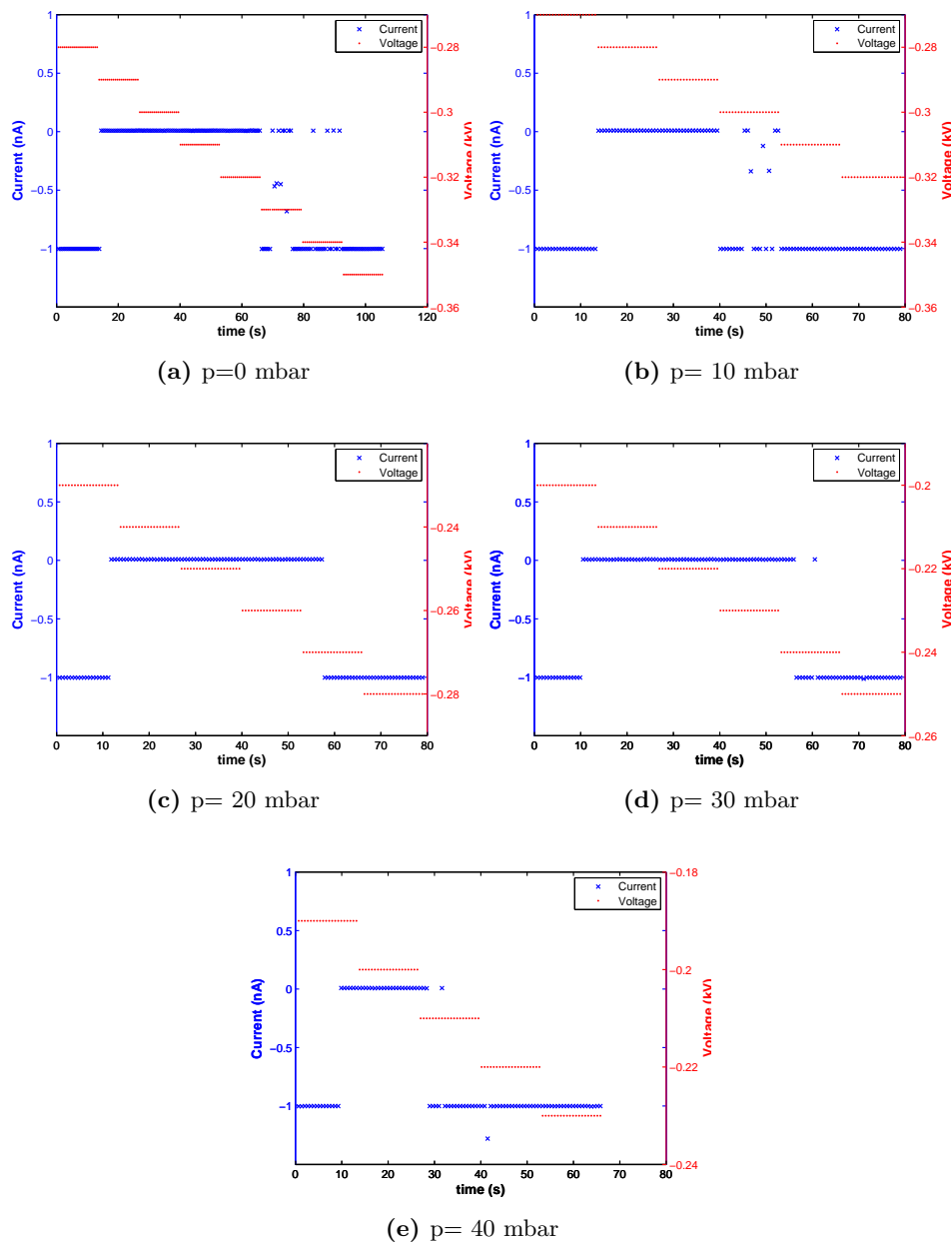


**Figure 4.19** – Measurements with voltage steps of 10 V at various pressures. It can be observed that the onset voltages are significantly lower than at  $d = 31\mu\text{m}$ .

Unfortunately the 50mbar measurement was not possible to carry out at a tip-electrode distance of  $20\mu\text{m}$ . The meniscus grows too much when applying this pressure which causes a fluidic connection between the tip and the electrode. An enormous flow rate is started causing the whole capillary

to be imbued with liquid. Images similar to Figure 4.13 were observed. No proper measurements were possible.

### Onset voltage as a function of pressure

From all measurements from the previous sections the onset voltage as a function of pressure can be determined. By taking the mean value of the five measurements per pressure - gap distance combination an average onset voltage can be plotted.

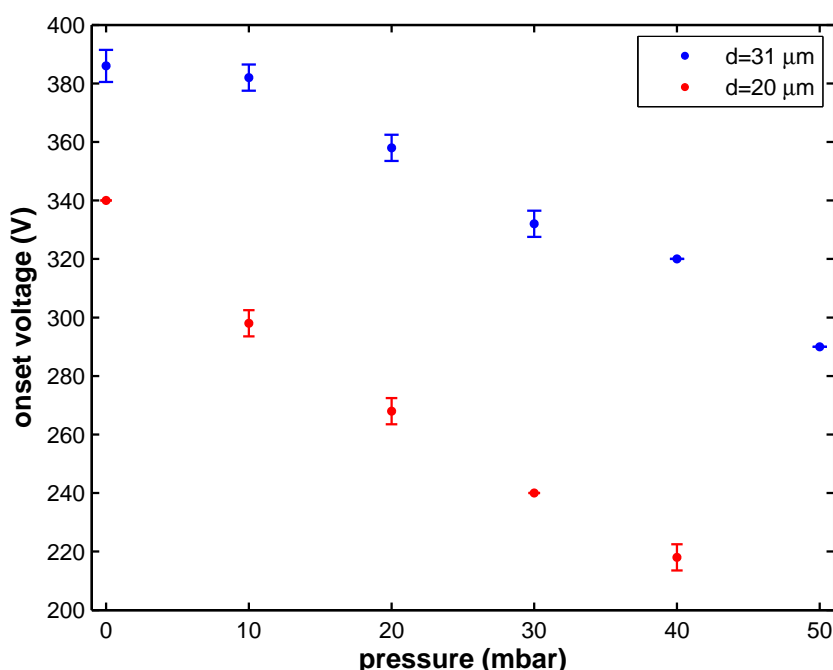


**Figure 4.20** – The onset voltage as a function of pressure. The error bars represent the standard deviation in the five measurements per pressure - gap distance combination.

### 1 μm capillary

The 10 μm capillary showed clear behavior: the current was either (almost) zero or it hit the compliance. The electrospray could be followed by the microscope. The onset voltage was well defined as the point at which the current hits the compliance and it could be determined with a precision of approximately 10V.

As the 1 μm has a 10 times small diameter the resistance is 10.000 times bigger. So the flow rate (and therefore) the current will be a lot smaller.

Also, the smaller dimensions make it much harder to follow the electrospray process by the microscope. A meniscus cannot be seen so it's hard to see whether the capillary is filled. To prevent the capillary from emptying no measurements were performed at zero pressure. The pressure can fluctuate a couple of mbars when setting it and the excess pressure must be greater than zero to maintain the capillary filled.

The onset voltage will not be as distinguishable as for the 10  $\mu\text{m}$  capillary so measuring in steps of 10V will not gain a lot of information. Therefore only a scope of 0 to 1100 V with a step of 100 V has been applied. To clarify the behavior of the capillary anyhow, in addition to the voltage and current-time characteristics also current-voltage plots have been included.

1  $\mu\text{m}$  capillary -  $d = 10\mu\text{m}$

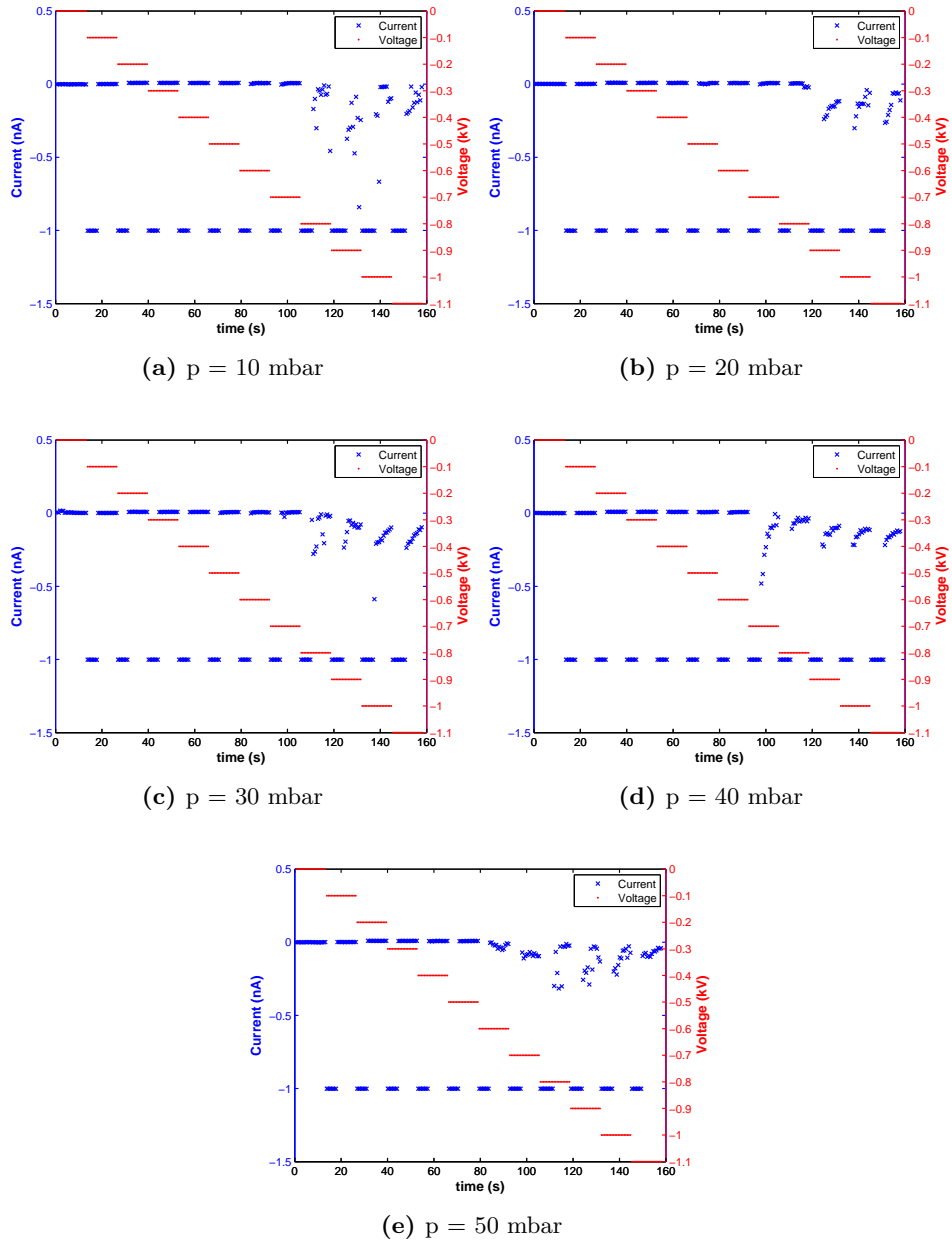


**Figure 4.21** – The capacitive part of the setup is still visible. Even though the current does not hit the compliance the onset voltage can be determined more or less as the point at which several consecutive current values are nonzero.

To interpret the current as a function of voltage I-V characteristics have also been plotted. The source measurement unit measures several currents per voltage step. The average of these measurements has been displayed. However, the compliance currents due to the capacitive function of the setup distort the average. Therefore a script has been written to filter these currents (also refer to chapter 8). To get a feeling for the dispersion of the measurement values the standard deviation in current measurements per voltage step has been plotted with error bars.

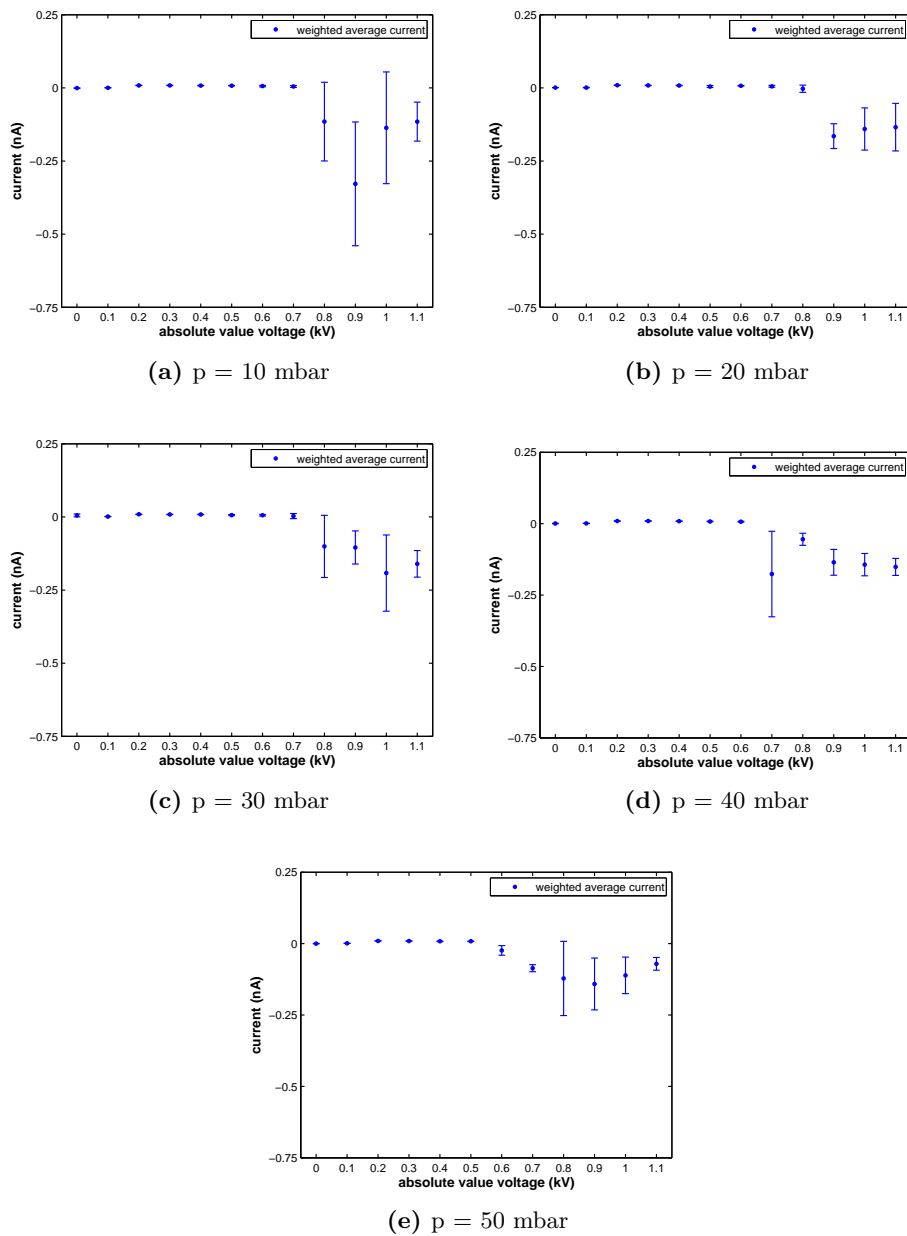
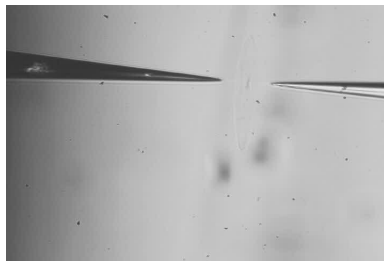


**Figure 4.22** – I-V characteristics of the capillary. The behavior of the current as a function of voltage can be studied well. In order to have a good average the compliance currents of -1 nA due to the capacitive function have not been taken into account in calculating the average current and standard deviation. Note that for convenience of reading from left to right the absolute value of the voltage has been used.



(a)



(b)



(c)

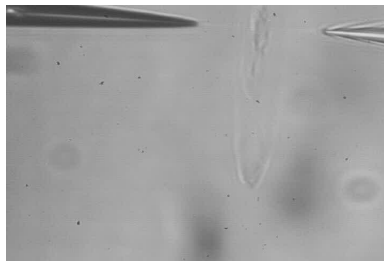


(d)



(e)

**Figure 4.23** – Microscope captions with 20x magnification. At (a) the image as it is seen from the microscope has been shown. From (b) to (e) close ups are shown. Even though no Taylor cone or jet is visible, it can be observed some liquid hits the counter electrode. The 'pool' of liquid on the counter electrode changes from (b) to (e). In a movie this is clearer to observe than in static frames as presented here. This motion is not observed until the current increases. Again, this is a proof electro spray and not solely breakdown occurs.



(a)



(b)



(c)



(d)



(e)

**Figure 4.24** – Microscope image with 50x magnification. From (b) to (e) closeups are displayed. Even though these pictures show a 2.5 times greater magnification neither the Taylor cone nor capillary aperture is visible.

1  $\mu\text{m}$  capillary -  $d = 20\mu\text{m}$

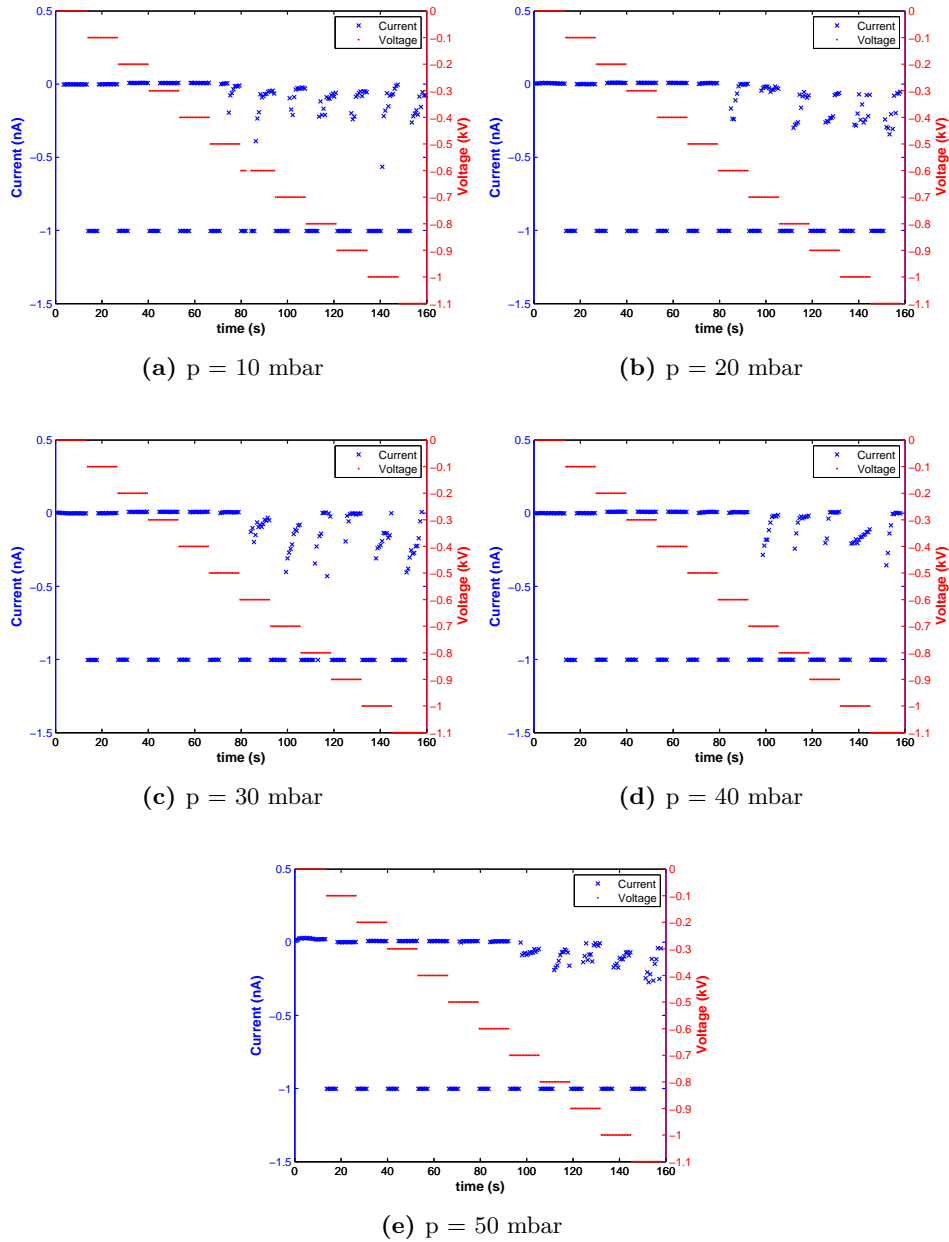
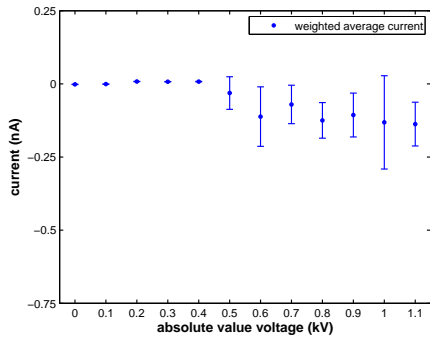
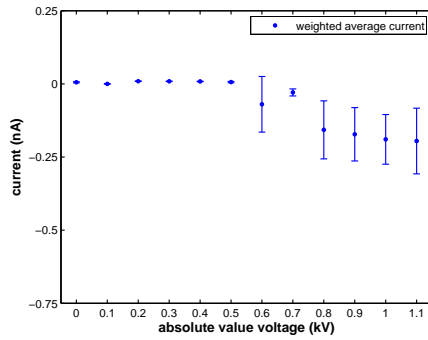


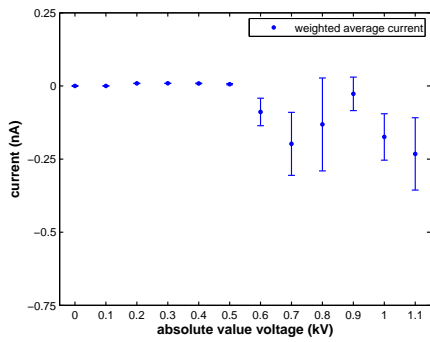
**Figure 4.25** – It’s interesting to observe that, unlike expected, it looks like the onset voltage is *increasing* with increasing pressure instead of decreasing. Also the onset voltage seems to be lower than at  $d = 10\mu\text{m}$  which may be called remarkable.



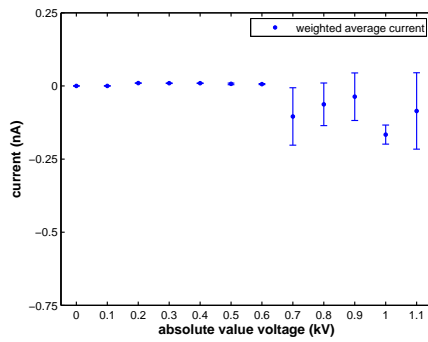
(a)  $p = 10$  mbar



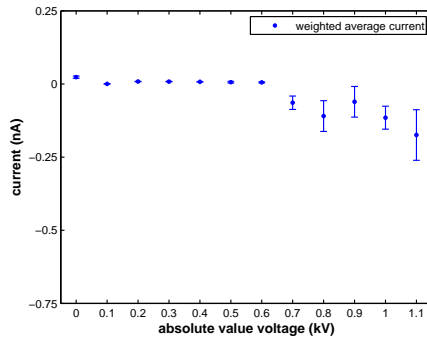
(b)  $p = 20$  mbar



(c)  $p = 30$  mbar



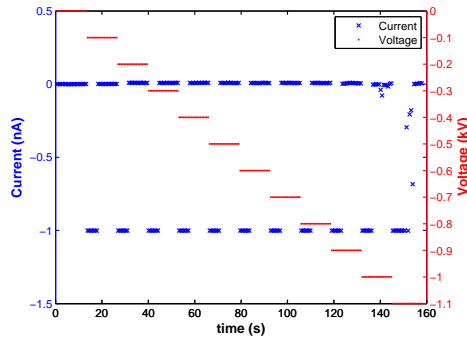
(d)  $p = 40$  mbar



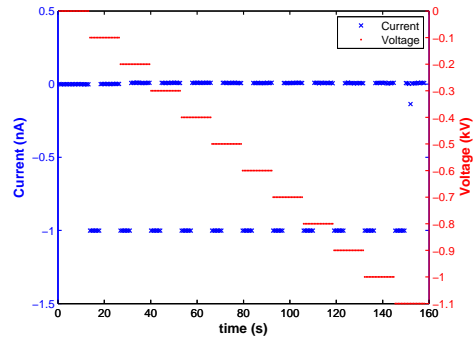
(e)  $p = 50$  mbar

Figure 4.26 – I-V characteristics of the capillary.

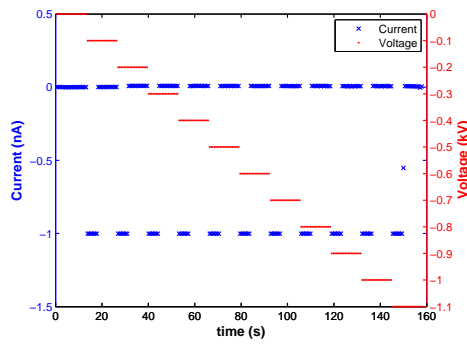
1  $\mu\text{m}$  capillary -  $d = 30\mu\text{m}$



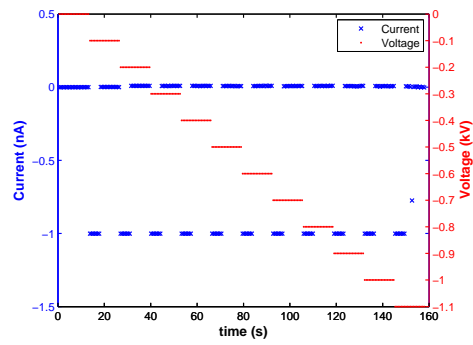
(a)  $p = 10$  mbar



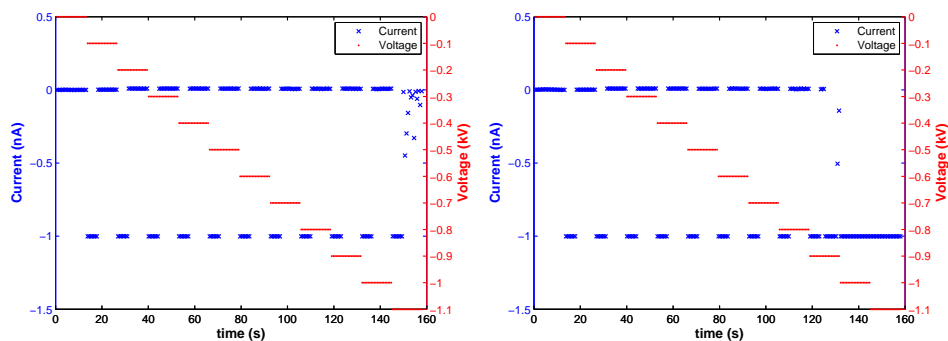
(b)  $p = 20$  mbar



(c)  $p = 30$  mbar

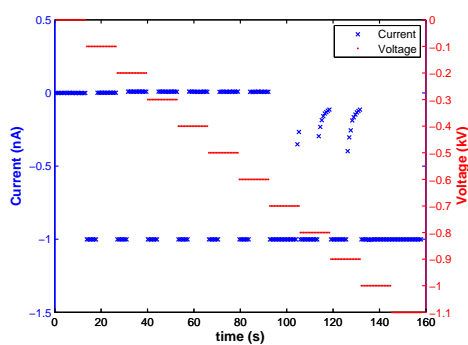


(d)  $p = 40$  mbar



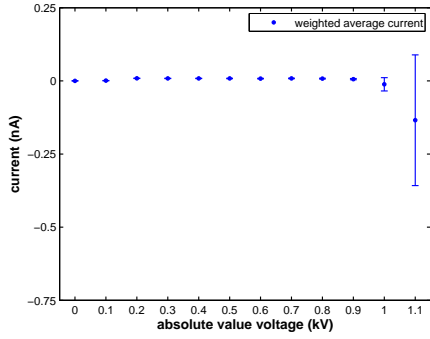
(e)  $p = 50$  mbar

(f)  $p = 250$  mbar

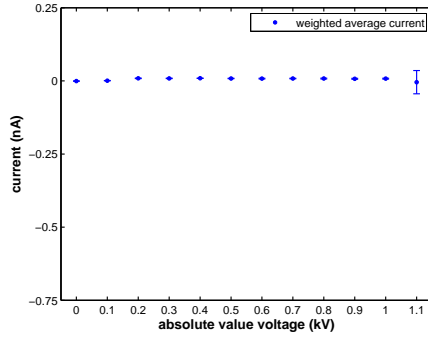


(g)  $p = 500$  mbar

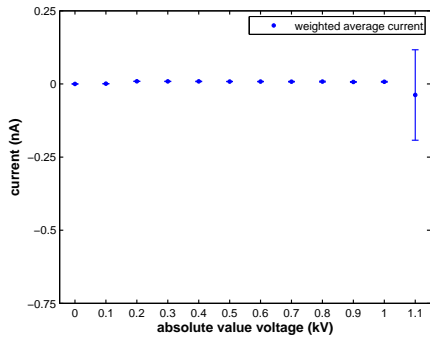
**Figure 4.27** – It looks like the onset voltage is slightly higher than 1100V for pressures from 10 to 40 mbar so it's hard to detect electro spray. To prove that pressure does affect the onset voltage very high pressures of 250 mbar and 500 mbar have been applied. This was not possible with the  $10 \mu\text{m}$  capillary as these pressures would exceed the Laplace pressure. This is not the case for the  $1 \mu\text{m}$  capillary. A decrease in onset voltage as the pressure increases can be observed.



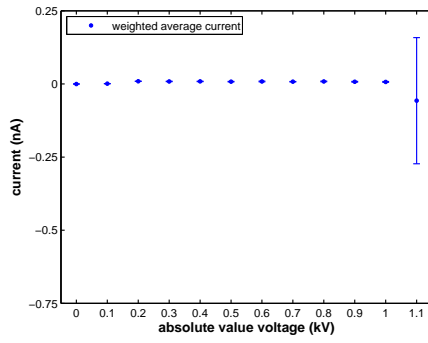
(a)  $p = 10$  mbar



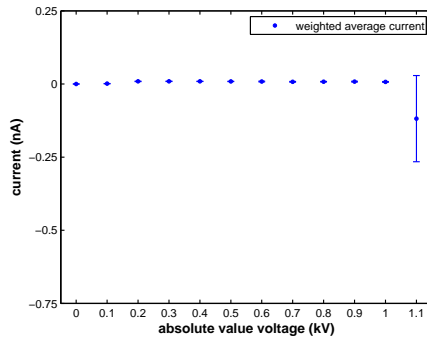
(b)  $p = 20$  mbar



(c)  $p = 30$  mbar



(d)  $p = 40$  mbar



(e)  $p = 50$  mbar

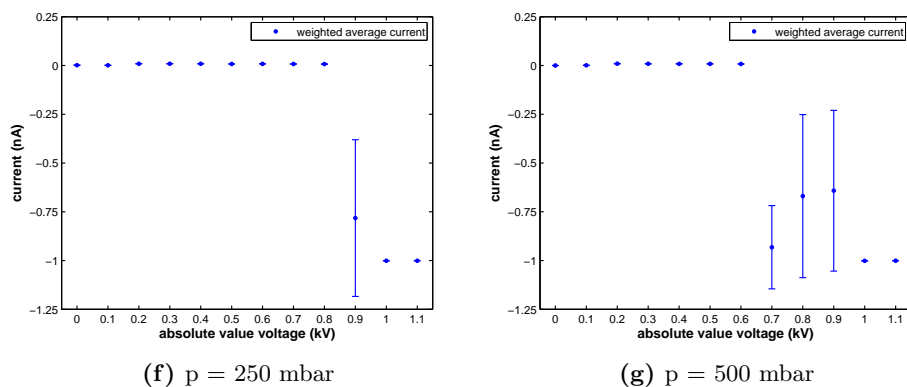


**Figure 4.28** – The lack of clear electrospray is visible from (a) to (e). However, increasing the pressure significantly up to 500 mbar does create electrospray. Note that the current axis at (f) and (g) is different from the other axis, because this is the first situation for the 1  $\mu\text{m}$  capillary the compliance is reached stably.

### Onset voltage as a function of pressure

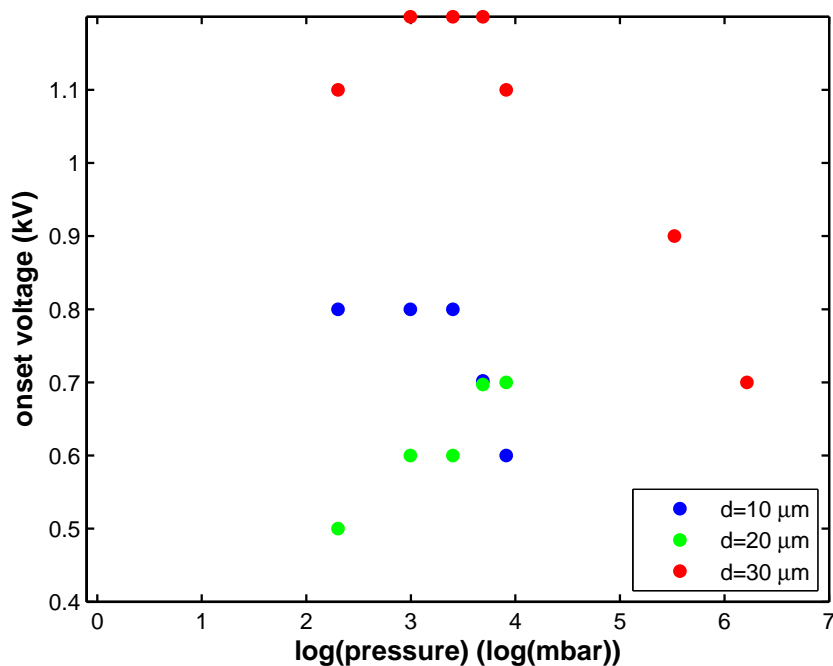


**Figure 4.29** – The onset voltage as a function of pressure. To view the onset voltages at 250 and 500 mbar pressure a semi logarithmic plot has been used. The voltage values for the 30  $\mu\text{m}$  capillary (red) on the very top of the plot represent onset voltages which exceed 1.1 kV.

This plot does not really correspond to expected values. At least it is expected that the onset voltage drops with increasing pressure. Both the 10  $\mu\text{m}$  and 30  $\mu\text{m}$  distances satisfy this hypothesis, but the 20  $\mu\text{m}$  one clearly does not. It may look like the onset voltage for 30  $\mu\text{m}$  distance is increasing from 10 to 20 mbar, but defining the onset voltage is not as obvious as it was for the 10  $\mu\text{m}$  capillary. It depends on the observer whether the couple of nonzero currents at 10 mbar pressure (refer to the I-V characteristics) are regarded as electrospray currents (i.e. the onset voltage has been reached) or not.

Nevertheless, the onset voltage for 20  $\mu\text{m}$  is clearly increasing with increasing pressure. This does not correspond to theoretical predictions at all.

## Chapter 5

# Data analysis

The effects of pressure on the onset voltage have been studied. It is expected that applying an excess pressure will make the the onset voltage drop as this extra applied pressure will decrease the 'effective' Laplace pressure. For a situation without excess pressure the equilibrium between the Maxwell stress, i.e. the stress generated by the applied voltage, and the capillary pressure (Laplace pressure) reads:<sup>13</sup>

$$\frac{1}{2}\epsilon_0 E^2 = \frac{2\gamma \cos(\theta_T)}{R} \quad (5.1)$$

Applying an excess pressure  $p_{\text{ex}}$  will lead to an equilibrium:

$$\frac{1}{2}\epsilon_0 E^2 = \frac{2\gamma \cos(\theta_T)}{R} - p_{\text{ex}} \quad (5.2)$$

Next, the potential  $V$  is defined as the integral over the electric field.

$$V = \int_{\text{tip}}^{\text{electrode}} \vec{E} \cdot d\vec{r} \quad (5.3)$$

It is assumed the way the electric field decreases between the tip and the counter electrode is not a function of the applied voltages. So if  $E$  decreases by  $1/r$  if 100 V is applied, it will still decay by this rate if 200 V is applied. Therefore, a linear relation between voltage and electric field is taken. Hence, Equation 5.2 can be rewritten as

$$\frac{1}{2}\epsilon_0 \frac{V^2}{k} = \frac{2\gamma \cos(\theta_T)}{R} - p_{\text{ex}} \quad (5.4)$$

In which  $k$  denotes a constant. Using this expression the behavior of the voltage and therefore onset voltage can be described.

$$V = \sqrt{\frac{2k}{\epsilon_0} \left( \frac{2\gamma \cos(\theta_T)}{R} - p_{\text{ex}} \right)} \quad (5.5)$$

$$V_{\text{on}}(p_{\text{ex}}) \propto \sqrt{b - c \cdot p_{\text{ex}}} \quad (5.6)$$

In which  $b$  and  $c$  are constants. So the onset voltage is expected to be proportional to the square root of the excess pressure. However, letting MATLAB determine the best fit learns a quadratic one seems to fit best. Both a quadratic and square root fit have been plotted in Figure 5.1.

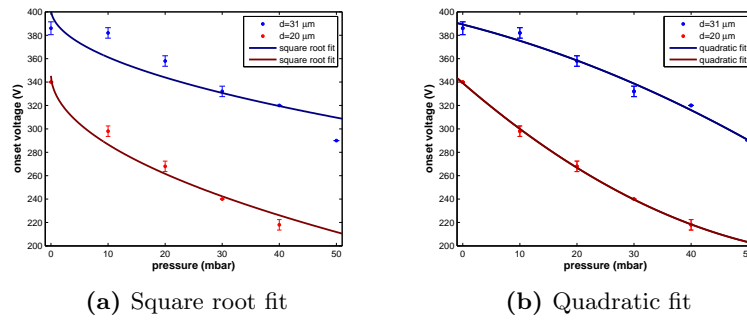


**Figure 5.1** – It can be observed the quadratic fit is much better than the square root fit. However, whereas the quadratic fit gives a cone up parabola for  $31 \mu\text{m}$  distance and a cone down one for  $d = 20 \mu\text{m}$ , the square root fit gives similar shapes for both distances.

Both fits have been generated by MATLAB automatically. However, trying to fit a function in the shape of Equation 5.5 by hand yields much better fits, as shown by Figure 5.2.

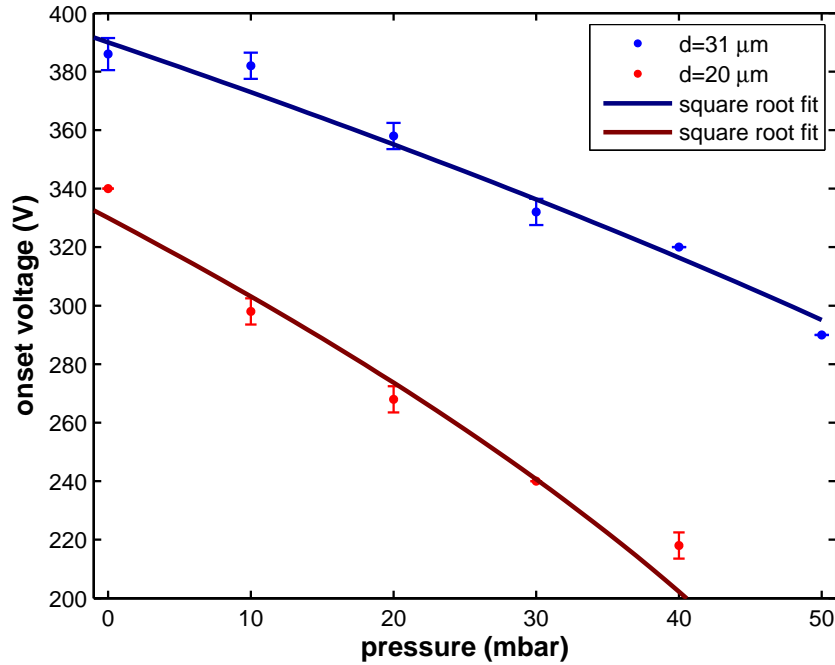


**Figure 5.2** – A fit of the form  $a\sqrt{b(c-p)}$  fits the data points well, especially for 31  $\mu\text{m}$  distance.

A function of this form gives a proper fit. In addition, this fit satisfies the theoretical predictions and for both distances it gives the same shape (so not a cone up and cone down parabola for example). The fact that the curve is decreasing as the pressure is increasing is also plausible: at a certain point the applied pressure equals the Laplace pressure so no voltage is needed to start the 'spraying process'. Therefore, both curves should go to zero at a certain point, which is the case (refer to Figure 5.3).

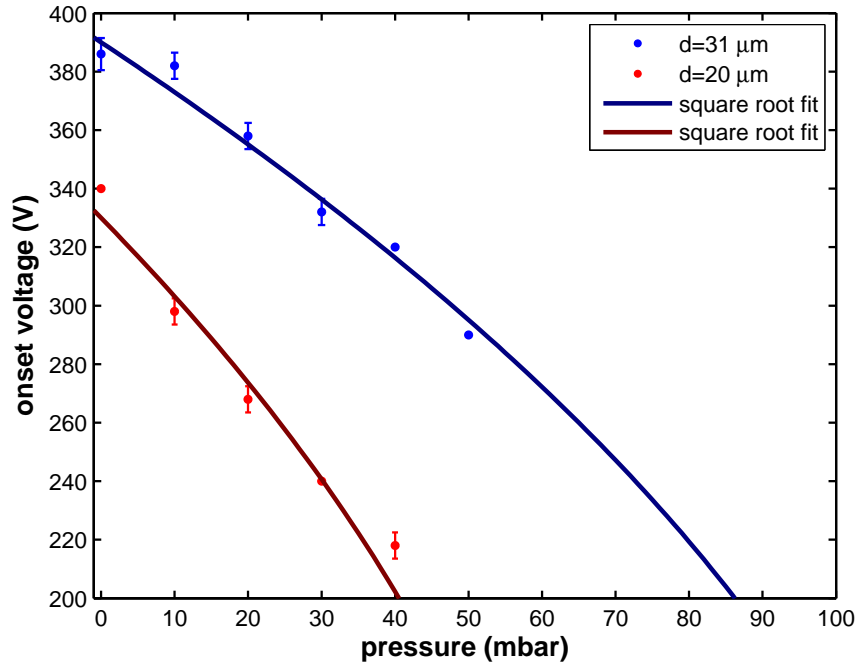


**Figure 5.3** – When the pressure axis is extended, the zeros can be observed.

Even though the fit as presented in Figure 5.2 corresponds to theoretical predictions and suits the data points well, it is not perfect. Especially the fit for 20  $\mu\text{m}$  is not very accurate. A possible explanation may lie in the fact that the shape of the Taylor cone could be pressure dependent. This would alter Equation 5.2 and therefore the shape of the pressure - onset voltage characteristic. In addition, even though measurements at five different pressures per tip-electrode distance is sufficient to study the pressure dependence, measuring at even more pressures will make it easier to make an accurate fit.

Trying to make a proper fit for the 1  $\mu\text{m}$  capillary will not provide more insight due to the behavior deviating from theoretical models and the lack of sufficient data points.

## Chapter 6

# Conclusions

A setup satisfying all design requirements has been constructed. It has been demonstrated that electrospray from glass capillaries is possible for a capillary with  $10\ \mu\text{m}$  aperture at 20 and  $30\ \mu\text{m}$  capillary-electrode distance and for  $1\ \mu\text{m}$  aperture at 10, 20 and  $30\ \mu\text{m}$  distance. The lowest onset voltage has been measured with a  $10\ \mu\text{m}$  capillary at  $d = 20\ \mu\text{m}$  and an applied pressure of 40 mbar. This voltage reads 220 V, which still exceeds the aimed value of 100 V. Increasing the applied pressure clearly causes a decrease in onset voltage whereas increasing the capillary-electrode distance results in an *increase*. The obtained values satisfy theoretical predictions fairly well. For both the 10 and  $1\ \mu\text{m}$  capillary optical analysis have shown that electrospray rather than solely breakdown occurs.

Even though electrospray has been demonstrated for the  $1\ \mu\text{m}$  capillary, the behavior as function of pressure and capillary-electrode distance is not yet understood well. Further experiments are required to investigate this behavior. However, the possibility of creating electrospray at these dimensions has been demonstrated which brings the miniaturization of the electrospray process one step closer.

## Chapter 7

# Discussion and recommendations

Especially for the 10  $\mu\text{m}$  capillary it was not possible to measure I-V curves as the current immediately hit the compliance after the onset voltage was reached. This may be caused by the relatively large aperture (with respect to the tip-electrode distance). A high flow rate is therefore initiated easily. There is a suspicion this compliance causes the pulsating behavior of the Taylor cone. In order to obtain a stable cone-jet mode the compliance could have been increased, but this leads to an even higher (or *too* high) flow rate which causes even worse problems in turn. Even though high flow rates were not only observed in nonzero pressure configurations, applying an excess pressure will at least not help to bring down the flow rate.

Even though it has been demonstrated that electrospray occurs by identifying droplets on the counter electrode, the actual jet has hardly been observed. Only the captions of the 300  $\mu\text{m}$  needle show some sort of jet, but these measurements were only performed to visualize the process. A Taylor cone can be observed in the 10  $\mu\text{m}$  capillary measurements, but the jet cannot. Due to the small dimensions and the finite resolution of the microscope it was not possible to verify whether the Taylor cone indeed had an angle of  $49.3^\circ$ . Whereas for the 10  $\mu\text{m}$  capillary it was possible to see the meniscus (and visualize the growth if the applied pressure increased), it was not the case for the 1  $\mu\text{m}$  capillary at all. Therefore, the electrospray process was harder to follow at this dimension.

A consequence of reducing distances is the fact that the tip-electrode distance is not much bigger than the capillary radius. Most theoretical models discussed in this report do however only hold under this assumption. In addition, if the applied voltage increases the meniscus grows. Therefore, the liquid comes closer to the electrode. For large tip-electrode distances this

effect is negligible, but for the dimensions worked with in this study this is not just the case.

Electrospray has been demonstrated for the 1  $\mu\text{m}$  capillary, but the way the spraying process behaves as a function of pressure and capillary-electrode distance can be characterized as remarkable. Even though the liquid has been filtered using a filter with 0.2  $\mu\text{m}$  pores still some dirt particles could be seen inside the capillary. These could have originated from the ambient air as the capillary is held in air before being mounted to the syringe. It is suspected that these dirt particles do not play an important role in the 10  $\mu\text{m}$  capillary, but they do in the 1  $\mu\text{m}$  one. The presence of these particles may explain the notable behavior partly, but it remains strange. More experiments need to be performed to study this regime accurately.

Difficulties were also encountered in filling the capillaries. Applying a relatively high pressure and having patience was sufficient to fill the 1  $\mu\text{m}$  capillary. However, it was virtually impossible to fill the 100 nm capillary. The problems encountered with the 1  $\mu\text{m}$  capillary are only worse for the 100 nm one. The channel is 10 times smaller so any dirt particle will distort the process completely. Next, the resistance of the capillary is 10.000 times higher. Visualizing the 100 nm tip with the microscope used in this study will be virtually impossible, let alone seeing the Taylor cone.

Even though several measurements have been performed for the 10  $\mu\text{m}$  capillary, more measurements (especially various tip-electrode distances) could be performed to identify the process better. Due to the lack of supply of 10  $\mu\text{m}$  capillaries these measurements have not been performed. Initially only orienting measurements would be carried out with the 1  $\mu\text{m}$  capillary. Therefore only a limited number of measurements has been performed for this aperture. The number could be increased to study the behavior better.

The results show a decrease in onset voltage with an increasing applied pressure. In possible future configurations where electrical breakdown will prevent the setup from electro spraying, next to obvious improvements like minimizing surface tension and making the liquid as clean as possible, this pressure dependency could be used to lower the onset voltage. This method might make it possible to make the onset voltage lower than the breakdown voltage. When going to (sub) micrometer apertures the tip and therefore Taylor cone and jet will be even harder to visualize. In addition, the flow rate will be much lower than for a 10  $\mu\text{m}$  capillary. Optical verification of actual electro spray will be harder to perform. Therefore, better visualization method should be developed to study electro spray at these dimensions.

## Acknowledgments

I would like to thank Niels Tas and Joël Geerlings for supervising the assignment and providing good ideas, Remco Sanders for his creativity in finding practical solutions and Ruud van Damme for keeping an eye on the report.

I would also like to thank Hidde Dijkstra for his input (in particular Lab-View assistance) as well as fellow TST students for useful discussions during lunch break.

## Nomenclature

---

$d$	tip-electrode distance	$m$
$r_e$	capillary radius	$m$
$\theta_T$	Taylor cone angle, equals 49.3°	-
$V$	applied voltage	$V$
$V_{on}$	onset voltage	$V$
$E$	electric field	$V m^{-1}$
$\gamma$	surface tension	$N m^{-1}$
$\epsilon_0$	permittivity of vacuum, equals $8,854 \cdot 10^{-12}$	$F m^{-1}$
$q$	charge	$C$
$Z$	number (of charges)	-
$e$	elementary charge, equals $1.602 \cdot 10^{-19}$	$C$
$i_s$	(electrospray) current	$A$
$\epsilon_r$	relative permittivity	-
$\sigma$	conductivity	$S m^{-1}$
$v_f$	flow rate	$m^3 s^{-1}$
$\rho$	density	$kg m^{-3}$
$V_b$	breakdown voltage	$V$
$\kappa$	second Townsend coefficient	-
$p$	pressure	$Pa$
$A$	Paschen constant	$Pa^{-1} m^{-1}$
$B$	Paschen constant	$V Pa^{-1} m^{-1}$
$R_j$	Jet radius	$m$
$T$	temperature	$K$
$E_f$	Fermi level	$eV$
$E_{free}$	Energy at which electrons be- come free	$eV$
$T$	temperature	$K$
$\mathcal{E}_n$	energy of state $n$	$eV$
$k$	Boltzmann constant, equals $1.38065 \cdot 10^{-23}$	$m^2 kg s^{-2} K^{-1}$
$\delta$	droplet diameter	$m$
$\mu$	dynamic viscosity	$Pa s$
$r$	radius (in general)	$m$
$L$	length	$m$
$Q$	volume flow	$m^3 s^{-1}$
$R_V$	flow resistance	$Pa s m^{-3}$
$p_{amb}$	ambient pressure	$Pa$
$R$	curvature	$m$

---

# Bibliography

- [1] N. B. Cech and C. G. Enke, “Practical implications of some recent studies in electrospray ionization fundamentals,” *Mass Spectrometry Reviews*, vol. 20, pp. 362 – 387, 2001.
- [2] M. S. Wilm and M. Mann, “Electrospray and Taylor-cone theory, dole’s beam of macromolecules at last?,” *International Journal of Mass Spectrometry and Ion Processes*, vol. 136, pp. 167–180, 1994.
- [3] T. C. Rohner and H. H. Girault, “Electrochemical and theoretical aspects of electrospray ionization,” *Physical Chemistry Chemical Physics (PCCP)*, vol. 6, pp. 3056–3068, 2004.
- [4] B. R. Marija Radmilovic-Radjenovica, “The influence of ion-enhanced field emission on the high-frequency breakdown in microgaps,” *Plasma Sources Sci. Technol.*, vol. 16, pp. 337–340, 2007.
- [5] G. Taylor, “Disintegration of water drops in an electric field,” *Proceedings of the Royal Society of London, Series A. Mathematical and Physical Sciences*, vol. 208, no. 1382, pp. 383–397, 1964.
- [6] A. Jaworek and A. Sobczyk, “Electrospraying route to nanotechnology: an overview,” *Journal of Electrostatics*, pp. 197–219, 2008.
- [7] J. B. Fenn, “Electrospray ionization for mass spectrometry of large biomolecules,” *Science*, vol. 246, pp. 164–71, 1989.
- [8] A. Barrero and I. Loscertales, “Micro- and nanoparticles via capillary flows,” *Annu. Rev. Fluid Mech.*, vol. 39, pp. 89–106, 2007.
- [9] P. Kebarle and U. H. Verkerk, “Electrospray: from ions in solution to ions in the gas phase; what we know now,” *Mass Spectrometry Reviews*, vol. 28, pp. 898–917, 2009.
- [10] D. P. Smith, “The electrohydrodynamic atomization of liquids,” *IEEE Transactions on Industry Applications*, vol. IA-22, pp. 527–535, 1986.

- [11] K. T. A.R. Jones, “The production of charged monodisperse fuel droplets by electrical dispersion,” *J. Phys. D: Appl. Phys*, vol. 4, pp. 1159–1166, 1971.
- [12] G. H. L.B. Loeb, A.F. Kip, “Pulses in negative point-to-plane corona,” *Physical Review*, vol. 60, pp. 714–724, 1941.
- [13] C.-H. Chen, “Electrohydrodynamic stability,” *Department of Mechanical Engineering and Materials Science*, 2011.
- [14] D. Taffin, “Electric droplet fission and the rayleigh limit,” *Langmuir*, vol. 5, pp. 376–384, 1989.
- [15] J. Iribarne and B. Thomson *Journal of Chemical Physics*, vol. 64, p. 2287, 1976.
- [16] M. Dole *Journal of Chemical Physics*, vol. 49, p. 2240, 1968.
- [17] R. Pfeiffer and C. Hendricks, “Parametric studies of electro hydrodynamic spraying,” *AIAA J*, vol. 6, pp. 496–502, 1968.
- [18] J. de la Mora *Journal of Fluid Mechanics*, vol. 260, p. 155, 1994.
- [19] T.Ono, “Breakdown electric field strength between small electrode spacings in air,” *Journal of Micromechanics and Microengineering*, vol. 10, pp. 445–451, 2000.
- [20] F. Paschen, “Ueber die zum funkenbergang in luft, wasserstoff und kohlensure bei verschiedenen drucken erforderliche potentialdifferenz,” *Annalen der Physik*, vol. 273, pp. 69–96, 1889.
- [21] H. S. P. Carazzetti, Ph. Renaud, “Experimental study of electrical breakdown in mems devices with micrometer scale gaps,” *proc. of SPIE*, vol. 6884.
- [22] K. Burm, “Calculation of the townsend discharge coefficients and the paschen curve coefficients,” *Contrib. Plasma Phys.*, vol. 47, pp. 177–182, 2007.
- [23] J. R.S.Dhariwal and M. Desmulliez, “Electric field breakdown at micrometre separations in air and nitrogen at atmospheric pressure,” *IEE Proc.-Sci. Meas. Technol.*, vol. 147, 200.
- [24] J. Torres and R. Dhariwal, “Electric field breakdown at micrometre separation,” *Nanotechnology*, vol. 10, pp. 102–107, 1999.
- [25] R. Tirumala and D. Go, “Analytical formulation for the modified paschen’s curve,” *Applied Physics Letters*, vol. 97, 2010.

- [26] [http://www.ece.rochester.edu/courses/ECE234/MEMS\\_ESD.pdf](http://www.ece.rochester.edu/courses/ECE234/MEMS_ESD.pdf),  
“Electrical breakdown limits for mems,”
- [27] L. Tang and P. Kebarle, “Effect of the conductivity of the electro-sprayed solution on the electrospray current. factors determining analyte sensitivity in electrospray mass spectrometr,” *Anal. Chem.*, vol. 63, pp. 2709–2715, 1991.
- [28] G. Jackson and D. Duckworth, “Electrospray mass spectrometry of undiluted ionic liquids,” *Chem Comm*, pp. 522–523, 2004.
- [29] R. Hartman and D. Brunner, “Jet break-up in electrohydrodynamic atomization in the cone-jet mode,” *J. Aerosol Sci.*, vol. 31, pp. 65–95, 2000.
- [30] A. Ganan-Calvo, “New microfluidic technologies to generate respirable aerosols for medical applications,” *J. Aerosol Sci.*, vol. 18, pp. 249–275, 1997.
- [31] F. Menger, “Laplace pressure inside micelles,” *The Journal of Physical Chemistry*, vol. 83, p. 893, 1979.
- [32] B. Kirby, *Micro- and Nanoscale Fluid Mechanics: Transport in Microfluidic Devices*. <http://www.kirbyresearch.com/index.cfm/wrap/textbook/microfluidicsnanofluidics.html>: Cambridge University Press, 2010.
- [33] <http://commons.wikimedia.org/wiki/File:CapacitorHydraulicAnalogyAnimation.gif>, “Public domain,”
- [34] G. Vazquez and E. Alvarez, “Surface tension of alcohol + water from 20 to 50 c,” *J. Chem. Eng. Data*, vol. 40, pp. 611–614, 1995.
- [35] *Lange’s Handbook of Chemistry 10th ed.* 1967.

## Chapter 8

# Appendices

The following MATLAB script has been used to filter compliance currents and produce the I-V characteristics.

```
clear;
A=importdata('file.dat'); % import data
V=-A(:,1).*1E-3;
I=A(:,2).*1E9;
t=A(:,3);
l=0;
for k=1:length(I) % filter compliance currents due to capacitive charging
    if V(k)<1 % don't do this when the current actually hits the compliance
        if I(k)>-0.9
            l=l+1 ;
            nieuwI(l)=I(k);
            nieuwV(l)=V(k);
        end
    else
        l=l+1;
        nieuwI(l)=I(k);
        nieuwV(l)=V(k);
    end
end
end

Igem=zeros(1,12);
b=zeros(1,12);
x=1;
s=1;
mnieuwV(1)= nieuwV(1);
for k=1:length(nieuwV) % calculate average current per voltage step
    if k ~= length(nieuwV)
        if nieuwV(k) == nieuwV(k+1)
```

```

        nnieuwI(s) = nieuwI(k);
        s = s+1;
    else
        nnieuwI(s) = nieuwI(k);
        Igem(x)=mean(nnieuwI(1:s));
        b(x)=std(nnieuwI(1:s));
        x=x+1;
        s=1;
    end
end
else
    nnieuwI(s) = nieuwI(k);
    Igem(x)=mean(nnieuwI(1:s));
    s=1;
end
end

pa=errorbar(0:0.1:1.1,Igem,b,'ob') % make plot incl.
    errorbars with standarddeviation
set(pa,'LineWidth',2)

axis([0 1.1 -1.25 0.25]); % change plot layout settings
xlabel('absolute value voltage(v)', 'fontsize',12,'fontweight','b');
ylabel('current (nA)', 'fontsize',12,'fontweight','b');
set(gca,'LineWidth',1,'FontSize',10,'Ytick',-1.5:0.25:0.5,'Xtick',0:0.1:1.1);
l=legend('weighted average current','Location','NorthEast');
set(l,'fontsize',10);

```